Ferdowsi University of Mashhad

ISSN 2008-9147
Numbers: 21

JCMR

Journal of Cell and Molecular Research

Volume 11, Number 1, Summer 2019

بسم الله الرحمن الرحيم

Issuance License No. 124/902-27.05.2008 from Ministry of Culture and Islamic Guidance
Scientific Research Issuance License No. 161675 from the Ministry of Science, Research and Technology, Iran

Journal of Cell and Molecular Research (JCMR)

Volume 11, Number 1, Summer 2019

JCMR Office: Department of Biology, Faculty of Sciences, Ferdowsi University of Mashhad, Mashhad, Iran.
Postal Code: 9177948953
P.O. Box: 917751436
Tel: +98-513-8804063/+98-9156996326
Fax: +98-513-8795162
E-mail: jcmr@um.ac.ir
Online Submission: http://jcmr.um.ac.ir

Table of Contents

Journal of Cell and Molecular Research (2019) 11 (1), 1-7 DOI: 10.22067/jcmr.v11i1.78768

Research Article

Investigating the Effects of Morphine on Survival and Sensitivity to Cisplatin in Ovarian Cancer Cells

Maryam Rezaeigazik[1], Mohammad Nabiuni[2*], Hanieh Jalali[1], Majid Kabuli[3]

[1] *Department of Animal Biology, Faculty of Biological Sciences, Kharazmi University, Tehran, Iran*
[2] *Department of Cell and Molecular Biology, Faculty of Biological Sciences, Kharazmi University, Tehran, Iran*
[3] *Department of Medical Genetics, Faculty of Medicine, Tehran University of Medical Science, Tehran, Iran*

Received 23 January 2019 Accepted 17 May 2019

Abstract

Morphine as an analgesic drug is used frequently in cancer patients. Contradictory results have been achieved from previous studies related to morphine effects in different concentrations. In current study, we examined the effect of clinical concentrations of morphine on A2780Cp cell line related to ovarian cancer. Moreover, its effect on the cytotoxicity of cisplatin was investigated. A2780CP cells were cultured in RPMI1640 medium and treated with clinical doses of morphine alone or in combination with cisplatin. The rate of cell proliferation was measured using MTT assay, morphological changes of nuclei were revealed by 4′,6-diamidino-2-phenylindole (DAPI) staining, and expression of B-cell lymphoma 2 (Bcl-2) was measured using flowcytometry. MTT assay results showed clinical concentration of morphine had no effect on viability of A2780CP cells and toxicity of cisplatin. DAPI staining revealed no chromatin condensation in presence of morphine, and flowcytometry analysis showed that the expression of Bcl-2 in treated cells did not differ from control cells. In accordance with findings in other kinds of cancer, our results demonstrated that morphine did not interact with the function of cispatin in ovarian cancer. This finding can be considered in clinical applications of morphine.

***Keywords*:** morphine, ovarian cancer, apoptosis, cytotoxicity, cisplatin

Introduction

Ovarian cancer is the fifth leading cause of cancer death in the world. This type of cancer develops in one of 70 women in their lifetime. DNA-damaging agents such as Cis-diammine dichloroplatinum II (cisplatin) are used for the treatment of those who suffer from ovarian cancer (Gonzalez et al., 2001). Actually pain occurs in more than 80% of cancer patients which can take place as a result of cancer or chemotherapeutic drugs. Morphine is the most analgesic drug which is used to relieve pain resulted from such conditions (Hatsukari et al., 2007). It is usually injected to patients about 50-100 mg/day for a 70kg human (Gupta et al., 2002). The most part of injected morphine is metabolized into active glucuronide metabolites in the liver. Plasma concentration of free morphine was reported about 1 µg/ml and moreover about 96 µg/ml in a dead cancerous patient (Sarah et al., 2004).

Previous studies demonstrated that the effects of morphine on growth of cancer cells depends on morphine concentration or type of the cells (Gach et al., 2011). Investigations which used extremely high concentrations have revealed that morphine reduces the growth of cancer cells *in vitro* (Maneckjee et al., 1990, Naoko et al., 1996) or tumor weight *in vivo* (Harimaya et al., 2002). However, there are some reports which show that low concentration of morphine produces early apoptotic markers in HL-60 and A549 tumor cell lines (Hatsukari et al., 2007), reduces the growth of HT-29 cancer cells (Tegeder et al., 2003), and arrests cell cycle progress in MCF-7 cells (Chen et al., 2017). In addition, other studies have shown that plasma concentration of morphine stimulates microvascular endothelial cell proliferation and angiogenesis *in vivo* or *in vitro* (Gupta et al., 2002) and promotes the tumor growth in breast cancer (Bimonte et al., 2015). Concerning the interaction of morphine with chemotherapy drugs, it may cause drug interference with chemotherapy agents routinely used to treat cancers such as cisplatin or naloxon and may affect drug cytotoxicity depending on its dosage (Cao et al., 2016, Chen et al., 2017). In 2016, Cao *et al*. showed that morphine affects the antitumor activity of cisplatin on tumor growth in nasopharyngeal carcinoma CNE-2 xenografts in nude mice (Cao et al., 2016).

* Corresponding author's E-mail: *devbiokharazmi@gmail.com*

With respect to broad usage of morphine to relieve pain in patients with ovarian cancer, it is important to determine its exact mechanism of function, especially its effect on cancer cell viability and/or death and also its interference with chemotherapy drugs. Continuing the previous work, which examined the effect of high concentrations of morphine on ovarian cancer cells (Nabiuni et al. ,2015), in the current study we investigated the effect of clinical concentrations of morphine on ovarian cancer cell line A2780CP, and also studied its effect on the cytotoxicity of cisplatin. This is the first time that the effect of the plasma dose of morphine is being studied on an ovarian cancer cell line.

Materials and Methods

Cell culture and growth conditions

All experiments were performed on human ovarian cancer cell line A2780CP. Cells were purchased from NCBI (National Cell Bank of Iran, Pasteur Institute) and were cultured in RPMI-1640 (Gibco-Invitrogen, US) with 10% (v/v) Fetal Bovine Serum (FBS, Gibco-Invitrogen, US) and 1% antibiotics (100 U/ml penicillin and 100 mg/ml streptomycin) at 37˚C in a 5% (v/v) CO_2 and 95% humidified incubator. The medium was changed every 48 hours.

Chemicals

Morphine sulfate was purchased from Daroupakhsh Co. (Iran), cisplatin from Naprod (India), Dimethyl Sulfoxide (DMSO) from Gibco (US) and triton from Merck (US), 3-[4,5-dimethylthiazole-2-yl]-2,5 diphenyltetrazolium bromide (MTT) and 4',6-diamidino-2-phenylindole (DAPI) from Sigma (US), and antibodies from Abcam (UK).

MTT assay

In this study, 1-50 µg/ml of morphine was regarded as clinical or plasma concentrations. To determine the percentage of viable cells and the proliferation rate, MTT assay was performed. Briefly, cells were cultured in 24-well plates, treated with morphine (0.1, 1, 10, 20 and 50 µg/ml) or cisplatin (1-40 µg/ml) or combination of them (2 µg/ml of cisplatin; 2 and 20 µg/ml of morphine). After completion of the treatment time, 100µl of MTT was added to each well and incubated for 4 hours in darkness at 37˚C; then, the medium was removed and formazan crystals were dissolved in DMSO. Finally, the optical density was read by spectrophotometer at 570nm wavelength.

DAPI staining

To observe the morphological changes of the nucleus, DAPI staining was performed. Briefly, A2780CP cells were cultured in 24 well plates, treated with 1 µg/ml of morphine, washed with PBS and fixed in formalin 4% for 20 minutes at 4˚C. The cells were washed with PBS and permeabilized with Triton X-100 for 20 minutes at room temperature. After washing with PBS, DAPI (1%) was added to each well for 30 seconds in darkness and room temperature. The additional staining was removed and wells were washed with PBS carefully. Finally, 0.5 ml of PBS was added to each well and cells were observed with a fluorescent microscope.

Measuring the expression of Bcl-2 by flowcytometry

In order to detect the apoptotic or anti-apoptotic effect of morphine, the expression of Bcl-2, as an anti-apoptotic protein, was measured. To do so, the cells were treated with 1 µg/ml of morphine up to 120 hours. Then, they were trypsinized and washed with PBS and centrifuged for 5 minutes in 2000 rpm and then were fixed with formalin 4% for 15 minutes at room temperature. After washing, the cells were permeabilized to antibodies with triton X-100 (0.4% v/v) for 20 minutes at room temperature, washed with PBS and centrifuged, then blocked with bovine serum albumin (BSA) 2.5% w/v in tween-PBS 0.1% v/v (TPBS) for 30 minutes at room temperature. In the next step, cells were treated with 50 µl primary antibody diluted 1:100 in diluting buffer (BSA 0.25% in TPBS 0.1% v/v) for 2 hours at room temperature, washed with PBS and centrifuged. Then, cells were incubated with 50 µl fluorescein-labeled goat antibody against rabbit IgG diluted 1:30 with diluting buffer for 30 minutes at 37˚C in darkness. The
additional antibody was washed and finally, the expression of Bcl-2 was measured by Partec PAS instrument and the data were analyzed by flow max software (Partec, Germany).

Statistical analysis

All experiments were repeated three times. Results were analyzed using one-way ANOVA with InStat-3 software. Values were expressed as Mean±S.E.M and *p*-value of <0.05 was considered significant.

Results

Plasma concentrations of morphine did not change the viability of A2780CP cells.

The A2780CP cells were grown for 3 and 5 days with plasma concentrations of morphine (1-50 µg/ml). Investigation of cell viability showed that the cells which treated with plasma concentrations of morphine, proliferated as same as cells in the control group. Although cells which treated with 1 and 20 µg/ml of morphine proliferated more than untreated cells, statistical analysis showed that differences were not significant at *P*-value of 0.05 (Figure 1).

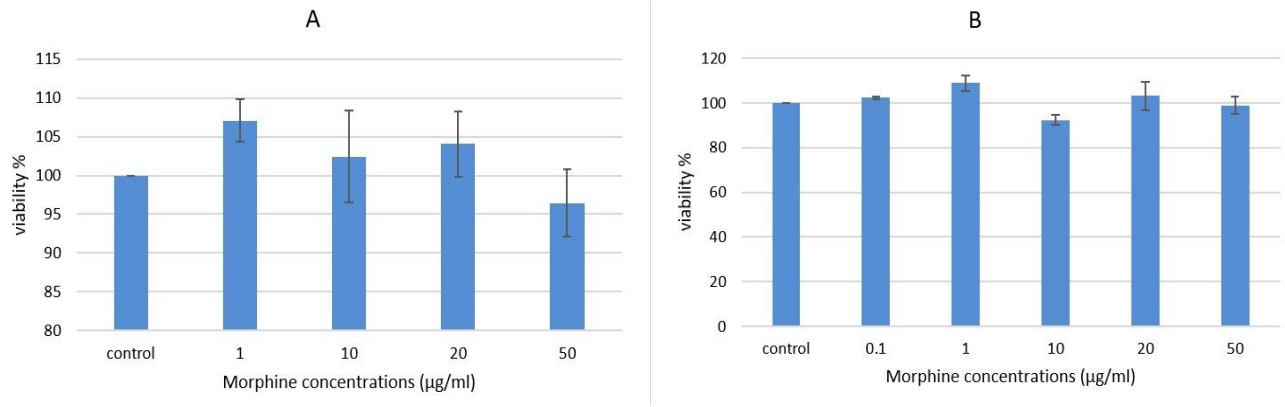

Figure 1. Percentage of viable cells under treatment with plasma concentrations of morphine compare to untreated cells after 3 days (A) and 5 days (B). The results are as Mean± SEM from three or more independent experiments.

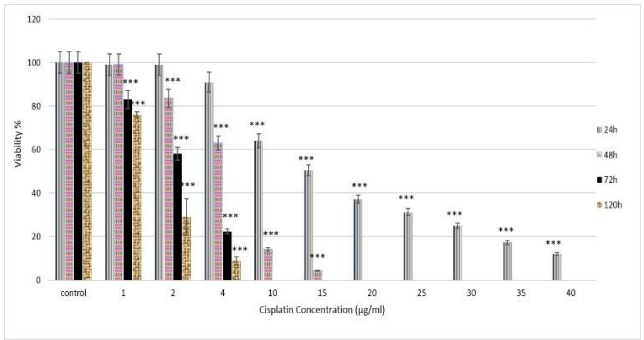

Figure 2. Percentage of viable cells under treatment with cisplatin. The results are as Mean± SEM from three independent experiments (* p<0.05, ** p<0.01, ***p<0.001).

The toxicity of cisplatin on A2780CP cells was not affected by morphine.

The effect of cisplatin (1-40 µg/ml) was examined by MTT assay after 1, 2, 3 or 5 days. As shown in Figure 2, cell viability was decreased after treatment with cisplatin in a dose and time-dependent manner. There was no viable cell after two days in doses more than 15 µg/ml. To evaluate the effect of morphine on the function of cisplatin, cells were treated with morphine and cisplatin. Co-treatment of the cells with 2 µg/ml of cisplatin in combination with 1 or 20 µg/ml of morphine showed that 20 µg/ml of morphine enhanced cytotoxicity of cisplatin slightly but not statically significant. The rate of cell viability in presence of 1 µg/ml of morphine and 2 µg/ml of cisplatin did not change compared to the cells which treated with 2 µg/ml of cisplatin (Figure 3).

Plasma concentration of morphine did not harm the nuclei of A2780CP cells.

DAPI staining was performed after 48 hours treatment of A2780CP cells with 1 µg/ml of morphine. Observation showed that the total number of nuclei in morphine treated cells was comparable with untreated cells and no fragmented nuclei were found in the presence of 1 µg/ml of morphine (Figure 4). These results were in accordance with MTT assay results.

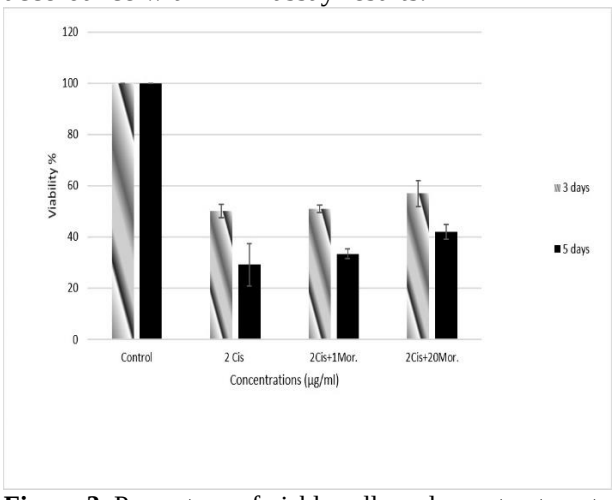

Figure 3. Percentage of viable cells under co-treatment with 2 µg/ml of cisplatin and 1 or 20 µg/ml of morphine. The results are as Mean± SEM from three independent experiments.

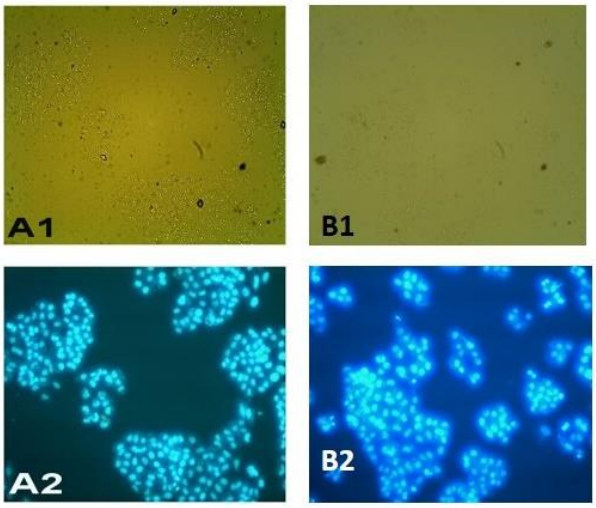

Figure 4. DAPI stained nuclei under light (part 1) and florescent (part 2) microscope. A: untreated (control), B: 1 µg/ml of morphine (× 100).

Anti-apoptotic Bcl-2 protein was expressed as control state

To investigate the effect of morphine on the function of apoptotic factors in A2780CP cells, the expression of Bcl-2 protein, as an anti-apoptotic protein, was evaluated. Briefly, cells were treated with predominant plasma concentration of morphine (1µg/ml) for 5 days. The results are shown in Figures 5. 1µg/ml of morphine enhanced the expression of Bcl-2 in the amount of 6.5%, so that the expression of Bcl-2 in control cells was 72.86% compared to 79.36% in morphine treated cells. The difference was not significant at P-value of 0.05.

Discussion

Several studies have shown that morphine administration can affect cancer cells growth (Bhat et al., 2004, Bimonte et al., 2013, Donahue et al., 2009); and there is some information about the mechanisms by which morphine acts through (Crawford and Bowen 2002, Diao et al., 2000, Donahue et al., 2009, Gach et al., 2011, Hsiao et al., 2009, Iglesias, 2003, Koodie et al., 2010). Morphine effects may be depend not only on the cell type and the system of investigation (*in vitro* or *in vivo*) but also on its doses. Investigation of high doses of morphine has been shown apoptotic cell death induction in a dose and time-dependent manner, however, these concentrations are not tolerable in animal bodies.

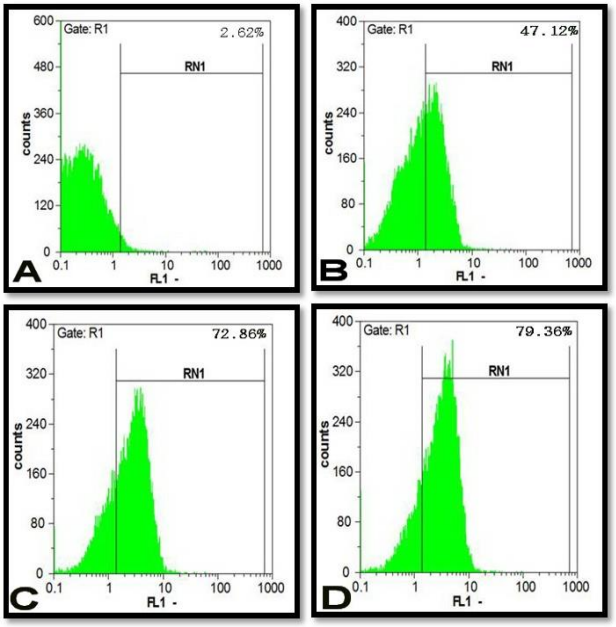

Figure 5. Measurement of Bcl-2 protein expression in the cells which treated with plasma concentration of morphine. A) Unstained, B) negative control, C) untreated (normal), D) cells treated with 1 µg/ml Morphine. The RN1 region shows the percentage of BCl-2 expression.

Herein, we studied the effect of clinical concentrations of morphine. Our findings showed that morphine did not increase the proliferation of A2780CP cells significantly in the range of 0.1-50 µg/ml, which was in agreement with Cao et al. findings which showed 0.1-100 µg/ml of morphine did not change the cell viability of human nasopharyngeal carcinoma CNE-2 cells significantly (Cao et al., 2016). Investigation of clinically relevant doses of morphine on human glioblastoma T98G cells (Lazarczyk et al., 2010) and human breast carcinoma cells (Bimonte et al., 2015) and bladder cancer cells (Harper et al., 2018) indicated that morphine increased proliferation of cancerous cells, that can be explained with differences in morphine concentration, duration of treatment and the type of cancer cells.

In the course of this study, we also examined the combined effect of morphine and cisplatin on A2780CP cell line. Cisplatin is a well-known DNA-damaging factor and is a common chemotherapeutic agent. It is used widely for head and neck, ovarian and non-small cell lung cancers. Previous studies have been demonstrated that cisplatin induces cell death through apoptosis and cell cycle regulating pathways (Agrez et al., 2011, Tanida et al., 2012). In previous study by Cao et al., it was indicated that morphine (1 µg/ml) abolished the 4 µg/ml cisplatin-induced loss of cell viability

only at 72 h, but not at 48 h; also, morphine (0.1 µg/ml, 10 µg/ml or 100 µg/ml) did not show any effect on the cisplatin-induced decrease in cell viability of CNE-2 cells at 24 h, 48 h and 72 h (Cao et al., 2016). In compare, our results showed that co-treatment of 1 and 20 µg/ml of morphine and 2 µg/ml of cisplatin did not lead to obvious increase in cell proliferation. From these findings, it can be concluded that the effects of morphine might be different based on cellular sensitivity or cisplatin dose.

Several investigations reported that high concentrations of morphine, induce apoptosis in cancer cells that are along with a decrease in Bcl-2 expression; which means morphine acts through an intrinsic pathway and promotes apoptosis (Cheng et al., 2006, Kapasi et al., 2004). On the other hand, studies in low doses of morphine have shown that morphine inhibits cell death with the inhibitory effect on the expression of p53 in MDA.MB231 cells (breast cancer cell line) (Bimonte et al., 2015) or through declining the expression of Bcl-2 in nasopharyngeal carcinoma (Cao et al., 2016). Although the combined treatment of morphine (1 µg/ml) and cisplatin (4 µg/ml) increased the expression of Bcl-2 in nasopharyngeal carcinoma cells (Cao et al., 2016), our finding indicated that in ovarian cancer cells, morphine did not have obvious effect on Bcl-2 expression in usual plasma concentration.

Conclusion

In conclusion, the present study demonstrated that plasma concentrations of morphine, in range of clinical doses, could not alter the proliferation of ovarian cancer cells and the cytotoxicity of cisplatin as well. In terms of its effect on the molecular pathway of apoptosis, morphine also did not affect the expression of anti-apoptotic factor, Bcl-2. These results can be considered for the potential effects of this drug in ovarian cancer patients.

Authors' contributions

All authors conceived design of study and basic concepts. MR and HJ performed laboratory tests and statistical analysis. All authors wrote the article and approved the final version of the manuscript.

Funding

No financial support.

Conflict of interest

The authors declare that they have no competing interests.

Ethical Statement

Not applicable.

Acknowledgements

We would like to thank Ms. Latifeh Karimzadeh for his kindly helps.

References

Agrez M., Garg M., Dorahy D. and Ackland S. (2011). Synergistic Anti-Tumor Effect of Cisplatin When Combined with an Anti-Src Kinase Integrin-Based Peptide. Journal of cancer therapy 02: 295-301.

Bhat R. S., Bhaskaran M., Mongia A., Hitosugi N. and Singhal P. C. (2004). Morphine-induced macrophage apoptosis: oxidative stress and strategies for modulation. Journal of leukocyte biology 75: 1131-1138.

Bimonte S., Barbieri A., Palma G. and Arra C. (2013). The role of morphine in animal models of human cancer: does morphine promote or inhibit the tumor growth? Biomed research international 2013: 258141.

Bimonte S., Barbieri A., Rea D., Palma G., Luciano A., Cuomo A., Arra C. and Izzo F. (2015). Morphine Promotes Tumor Angiogenesis and Increases Breast Cancer Progression. Biomed research international 2015: 161508.

Cao L. H., Li H. T., Lin W. Q., Tan H. Y., Xie L., Zhong Z. J. and Zhou J. H. (2016). Morphine, a potential antagonist of cisplatin cytotoxicity, inhibits cisplatin-induced apoptosis and suppression of tumor growth in nasopharyngeal carcinoma xenografts. Scientific reports 6: 18706.

Chen Y., Qin Y., Li L., Chen J., Zhang X. and Xie Y. (2017). Morphine Can Inhibit the Growth of Breast Cancer MCF-7 Cells by Arresting the Cell Cycle and Inducing Apoptosis. Biological and pharmaceutical bulletin 40: 1686-1692.

Cheng W. F., Chen L. K., Chen C. A., Chang M. C., Hsiao P. N., Su Y. N., Lee C. N., Jeng H. J., Hsieh C. Y. and Sun W. Z. (2006). Chimeric DNA Vaccine Reverses Morphine-Induced Immunosuppression and Tumorigenesis. Molecular therapy 13: 203-210.

Crawford K. W. and Bowen W.D. (2002). Sigma-2 Receptor Agonists Activate a Novel Apoptotic Pathway and Potentiate Antineoplastic Drugs in Breast Tumor Cell Lines. Cancer research 62:313–

322.

Diao C. T. M., Li L., Lau S. Y., Wong T. M. and Wong N. S. (2000). k-Opioid receptor potentiates apoptosis via a phospholipase C pathway in the CNE2 human epithelial tumor cell line. Biochimica et Biophysica Acta 1499:49-62.

Donahue R. N., McLaughlin P. J. and Zagon I. S. (2009). Cell proliferation of human ovarian cancer is regulated by the opioid growth factor-opioid growth factor receptor axis. American journal of physiology regulatory integrative Comparative physiology 296: R1716-R1725.

Gach K., Wyrębska A., Fichna J. and Janecka A. (2011). The role of morphine in regulation of cancer cell growth. Naunyn-Schmiedeberg's Arch Pharmacol 384: 221-230.

Gonzalez V. M., Fuertes M.A., Alonso C. and Perez J. M. (2001). Is cisplatin-induced cell death always produced by apoptosis? Molecular Pharmacology 59: 657-663.

Gupta K., Kshirsagar S., Chang L., Schwartz R., Law P. Y., Yee D. and Hebbel R. P. (2002). Morphine Stimulates Angiogenesis by Activating Proangiogenic and Survivalpromoting Signaling and Promotes Breast Tumor Growth. Cancer Research 62: 4491–4498.

Harimaya Y., Koizumi K., Andoh T., Nojima H., Kuraishi Y. and Saiki I. (2002). Potential ability of morphine to inhibit the adhesion, invasion and metastasis of metastatic colon 26-L5 carcinoma cells. Cancer Letters 187:121–127.

Harper P., Hald O., Lwaleed BA., Kyylay A., Johnston D., Cooper AJ. and Birch B. (2018). The impact of morphine treatment on bladder cancer cell proliferation and apoptosis: in vitro studies. Experimental oncology 40: 190-193.

Hatsukari I., Hitosugi N., Ohno R., Hashimoto K., Nakamura S., Satoh K., Nagasaka H., Matsumoto I. and Sakagami H. (2007). Induction of apoptosis by morphine in human tumor cell lines in vitro. Anticancer Research 27: 857-864.

Hsiao P. N., Chang M. C., Cheng W. F., Chen C. A., Lin H. W., Hsieh C. Y. and Sun W. Z. (2009). Morphine induces apoptosis of human endothelial cells through nitric oxide and reactive oxygen species pathways. Toxicology 256: 83-91.

Iglesias M. (2003). μ-opioid receptor activation prevents apoptosis following serum withdrawal in differentiated SH-SY5Y cells and cortical neurons via phosphatidylinositol 3-kinase. Neuropharmacology 44: 482-492.

Kapasi A. A., Coscia S. A., Pandya M. P. and Singhal P. C. (2004). Morphine modulates HIV-1 gp160-induced murine macrophage and human monocyte apoptosis by disparate ways. Journal of Neuroimmunology 148: 86-96.

Koodie L., Ramakrishnan S. and Roy S. (2010). Morphine Suppresses Tumor Angiogenesis through a HIF-1α/p38MAPK Pathway. American Journal of Pathology 177: 984-997.

Lazarczyk M., Matyja E. and Lipkowski A. W. (2010). A comparative study of morphine stimulation and biphalin inhibition of human glioblastoma T98G cell proliferation in vitro. Peptides 31: 1606-1612.

Maneckjee R., Biswas R. and Vonderhaar B. K. (1990). Binding of opioids to human MCF-7 breast cancer cells and their effects on growth. Cancer Reserch 50: 2234-2238.

Nabiuni M., Jalali H. and Rezaeigazik M. (2015). The effect of morphine on the proliferation of human ovarian epithelial cancer A2780cp cell line. International Journal of Cellular & Molecular Biotechnology 1-9.

Naoko S., Eisaburo S., Sachiko O. and Hirota F. (1996). Anti-cancer effects of morphine through inhibition of tumour necrosis factor-a release and mRNA expression. Carcinogenesis 17: 2337-2341.

Sarah K., Donna H. and Ginger B. (2004). Postmortem Morphine Concentrations Following Use of a Continuous Infusion Pum. Journal of analytical toxicology 28: 529-532.

Tanida S., Mizoshita T., Ozeki K., Tsukamoto H., Kamiya T., Kataoka H., Sakamuro D. and Joh T. (2012). Mechanisms of Cisplatin-Induced Apoptosis and of Cisplatin Sensitivity: Potential of BIN1 to Act as a Potent Predictor of Cisplatin Sensitivity in Gastric Cancer Treatment. International Journal of Surgical Oncology 2012: 862879.

Tegeder I., Gro¨sch S., Schmidtko A., Ha¨ussler A., Schmidt H., Niederberger E., Scholich K. and Geisslinger G. (2003). G Protein-independent G1 Cell Cycle Block and Apoptosis with Morphine in Adenocarcinoma Cells: Involvement of p53 Phosphorylation. Cancer Research 63: 1846–1852.

Journal of Cell and Molecular Research (2019) 11 (1),8-13 DOI: 10.22067/jcmr.v11i1.79988

Research Article

The Regulatory Effect of lncRNA PSORS1C3 on Different Variants of OCT4 in non-Pluripotent Cells

Fatemeh Mirzadeh Azad[1], Mahshid Malakootian[2], Seyed Javad Mowla[1*]

[1] *Department of Molecular Genetics, Faculty of Biological Sciences, Tarbiat Modares University, Tehran, Iran*
[2] *Cardiogenetic Research Center, Rajaie Cardiovascular Medical and Research Center, Iran University of Medical Sciences, Tehran, Iran*

Received 10 April 2019 Accepted 14 April 2019

Abstract

OCT4 is the major regulator of pluripotency in embryonic stem cells and its association with tumorigenesis, cellular stress response, and homeostatic multifactorial diseases have been recently reported. To serve the versatility in its function, OCT4 generates several transcript variants which their expression levels are tightly regulated through different mechanisms. PSORS1C3 is a long non-coding RNA with overlapping genomic location with OCT4 gene. Here, we investigated the effect of PSORS1C3 overexpression on OCT4 expression in different cell lines. Our data revealed that ectopic expression of PSORS1C3 did not affect OCT4 transcripts abundance in NT2 cells, as a model of pluripotent cells. However, in HEK293T cells, PSORS1C3 overexpression led to an increase in OCT4B as a homeostatic isoform and a decrease in OCT4A transcript level. We also observed that manipulating PSORS1C3 in HeLa cells, as a model of epithelial carcinoma line, caused an upregulation in OCT4A, OCT4C which could regulate stemness and proliferation and OCT4B transcripts at different time points. Our findings indicated that PSORS1C3 could affect the expression level of OCT4 spliced variants, according to their functions and the cells molecular context as well as genetic background. Considering these diverse regulatory effects and co-expression of OCT4 and PSORS1C3 in some cell lines, it is safe to consider PSORS1C3 as a modulator of OCT4 expression in non-pluripotent cells and in association with homeostatic pathways.

***Keywords*:** OCT4, PSORS1C3, expression regulation, lncRNA

Introduction

Oct4 is an octamer-binding transcription factor that regulates stemness, pluripotency and development (Campbell et al., 2007). As many stemness regulators play additional roles in tumorigenesis, OCT4 is also associated with cellular transformation, tumor invasion and drug resistance, and its expression alterations have been reported in many cancers (Atlasi et al., 2007; Du et al., 2009). Aside from its association with cancer, OCT4 is also linked with multifactorial diseases like psoriasis (Chang et al., 2007), inflammatory bowel diseases (Maragkoudaki et al., 2015), cardiovascular disorders (Lin et al., 2015) and major depressive disorder (Murphy et al., 2017) that share a common ground of deregulation in homeostatic pathways.

OCT4 has multiple spliced variants that each serves different functions at both RNA and protein levels (Gao et al., 2010; Li et al., 2015). OCT4A functions as a transcription factor and regulates stemness, cellular transformation and cell cycle. OCT4B and B1 show anti-apoptotic functions and are related to stress response and survival pathways (Asadi et al., 2011; Farashahi Yazd et al., 2011). The expression pattern of OCT4 transcripts varies in different cells, as well as during different biological events, where their expression levels are precisely regulated through different mechanisms (Wang and Dai, 2010; Rijlaarsdam et al., 2011).

Long non-coding RNAs (lncRNAs) are known as major regulatory factors capable of controlling gene expression at both transcriptional and post-transcriptional stages (Bhat et al., 2016). LncRNAs orchestrate the expression of their target genes through interactions with transcription machinery, chromatin remodelers and by acting as a guide, decoy or distributor of regulatory proteins or microRNAs (Engreitz et al., 2016). There are several reports on OCT4 expression regulation by lncRNAs in stem cells (Wang et al., 2013; Bai et al., 2015), however, the non-coding regulatory circuits that orchestrate OCT4 splicing in non-stem cells is not clearly identified.

PSORS1C3 is a lncRNA located upstream of OCT4 in the HLA-C locus which was first discovered in a

* Corresponding author's E-mail: *sjmowla@modares.ac.ir*

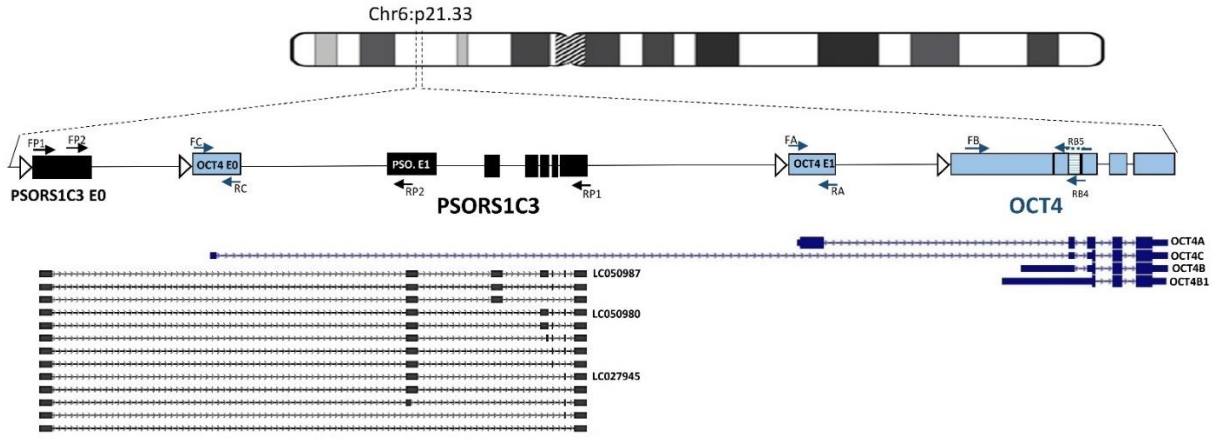

Figure 1. Schematic view of PSORS1C3-OCT4 locus and localization of primers which were used for cloning and gene expression quantification.

linkage analysis study on psoriasis (Holm et al., 2005). In our previous work, we reported a co-expression between PSORS1C3 canonical transcripts and OCT4 in different cells lines. By identifying a novel starting exon (exon 0) for both PSORS1C3 and OCT4, we demonstrated that these neighboring genes were physically entangled (Figure 1) (Malakootian et al., 2017). However, the expression screening indicated that PSORS1C3 longer variants which contained the transposon derived exon 0 had a fair co-expression with OCT4A mostly in non-pluripotent cells. Considering the significance of exonised transposon elements in biological pathways, we decided to investigate a possible regulatory effect of ectopic expression of PSORS1C3 long variants on OCT4 transcript level.

Materials and Methods

Constructing PSORS1C3 expressing vectors

PSORS1C3 long variants expressing vectors were constructed by cloning 3 of PSORS1C3 transcripts (LC050986, LC050987 and LC027945 (Figure1)) in pTracer-SV40 vector (Invitrogen, USA). Briefly, HepG2 and AGS cells (PSORS1C3 positive cell lines) were cultured to 70% confluency, as described before (Malakootian et al., 2017) and were lysed for RNA extraction with TRIzol reagent (Thermo Fisher Scientific, USA). Total RNA (2 µg) was treated with DNase I (Thermo Fisher Scientific, USA), then reversely transcribed using PrimeScript 1st Strand cDNA Synthesis Kit (TaKaRa, Japan), according to the manufacturer's protocol. PSORS1C3 long transcripts were amplified using FP1 and RP1 primers (Figure1, Table 1) by Pfu polymerase (GeneAll, South Korea) following the company's suggested protocol. Amplicons were purified using ExpinTM Combo GP kit (GeneAll, South Korea) and were directly cloned into pTracer-SV40 vector (Invitrogen, USA). The accuracy of the cloning and the identity of transcripts were confirmed by DNA sequencing (Macrogen, South Korea).

Cell transfection and targets expression analysis

HEK293T and HeLa cell lines were obtained from the Iranian biological resource center (IBRC, Iran). NTERA2c.D1 (NT2) cells were gifted by Dr. Peter Andrews. Cells were cultured in specific media as described before (Malakootian et al., 2017). Cells were seeded at 70% confluency and then transfection was done using Lipofectamine LTX (Thermo Fisher Scientific, USA) according to the manufacturer's instruction. In order to mimic PSORS1C3 natural expression, vectors containing 3 different variants were mixed for transfection. To determine the efficacy of transfection, cells were monitored for GFP signal emission, by fluorescent microscopy. Transfected cells were then lysed for RNA extraction 24 and 48 hours after transfection. After DNase I treatment and cDNA synthesis, real-time PCR was performed using target-specific primers (Table 1, Figure 1) and BioFACT™ 2X Real-Time PCR Master Mix (BioFACT, South Korea) to evaluate expression alterations in OCT4A, B, B1 and C transcript variants.

Results

PSORS1C3 was successfully overexpressed in different cell lines

24 hours after transfecting different cell lines with recombinant vectors containing three different isoforms of PSORS1C3, transfected cells were inspected by a fluorescent microscope and the

Table 1. Sequence of primers which were used in this study

Target name	Application	Primer name	Sequence
OCT4A	Real time PCR	FA	F:TCGCAAGCCCTCATTTC
		RA	R:CCATCACCTCCACCACCT
OCTB	Real time PCR	FB	F:AGACTATTCCTTGGGGCCACAC
		RB5	R:GGCTGAATACCTTCCCAAATAGA
OCT4B1	Real time PCR	FB	F:AGACTATTCCTTGGGGCCACAC
		RB4	R:CTTAGAGGGGAGATGCGGTCA
OCT4C	Real time PCR	FC	F:TGAGCGAGAAGCACGATCC
		RC	R:GGAACGAACCGTCGC C
PSORS1C3	Real time PCR	FP2	F:CCAGAGCAGCACGTAGCAG
		RP2	R:CCCTCCTTGCAGCATCATAAG
PSORS1C3	Transcript cloning	FP1	F: GTTTTGTCTGGGGCTCGTC
		RP1	R: CTTCACACACACCTTTATTATTAC

observed GFP signal indicated the efficacy of transfection (Figure 2A). Furthermore, we used qPCR (primers: FP2 and RP2) to evaluate the scale of overexpression in each cell line. Our analysis confirmed that PSORS1C3 was successfully overexpressed in transfected cells (Figure 2B).

PSORS1C3 ectopic expression had cell type specific effects on OCT4 transcripts

Ectopic expression of PSORS1C3 differentially affected each of the used cell lines. Accordingly, PSORS1C3 overexpression in NT2 cells did not affect OCT4 expression level significantly (Figure 3A), but the manipulation in HEK293T cells caused a downregulation in OCT4A expression (*p* value=0.008) and upregulation in OCT4B transcript (*p* value=0.042) since 24 hours post transfection (Figure 3B). In Hela cells, however, OCT4B level was increased only 48 hours after transfection (*p* value=0.023). The expression level of OCT4A and OCT4C were also significantly elevated (*p* value=0.041 and 0.02, respectively) after PSORS1C3 overexpression in Hela cells (Figure 3C).

Discussion

Cell type-specific expression of a gene is necessary for accurate functioning of signaling/homeostatic pathways and is commonly preserved by regulation at transcription level (Arvey et al., 2012). In particular, genes with several transcript variants show distinct patterns of expression for their variants in diverse cell types as well as during various biological events (Shi et al., 2017). The complex network of molecular regulators that manage the specificity of expression is different for each cell (Arvey et al., 2012), thus manipulating one of them could skew the network and differentially affect the target genes expression in each cell. According to our data PSORS1C3 ectopic expression could affect OCT4 expression, but the manifestation of the change in each OCT4 transcript variant was different in each tested cell line.

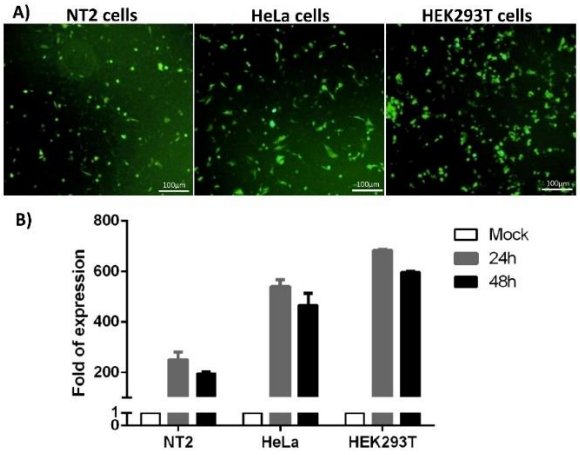

Figure 2. The efficacy and accuracy of transfection. A) The success of transfection was evaluated by visualizing GFP signal using a fluorescent microscopy, 24 h post transfection. B) Real-time PCR data confirmed the over expression of PSORS1C3 transcripts at 24 and 48 h post transfection.

As a teratocarcinoma cell line, NT2 needs and expresses high levels of OCT4A, B1(Atlasi et al., 2008) and C (Malakootian et al., 2017) that are needed for maintaining stemness state. The stemness-related regulatory pathways are strictly

regulated (Kelly and Gatie, 2017) and according to our findings,

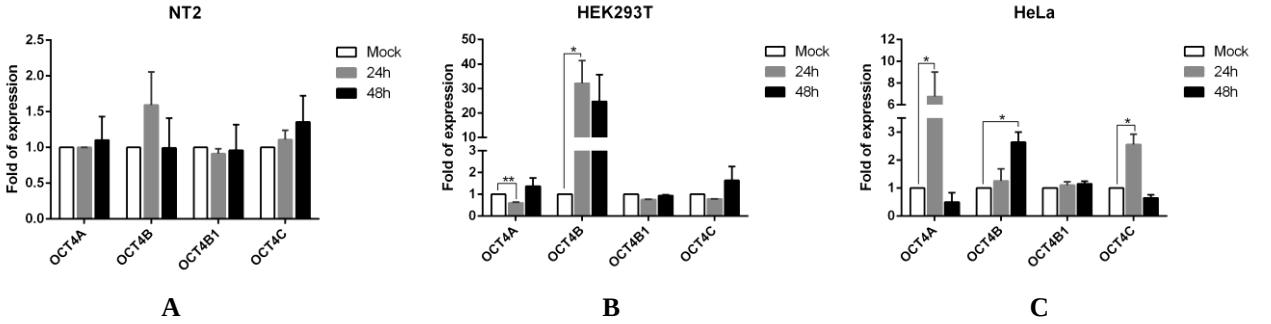

Figure 3. The effect of PSORS1C3 overexpression on OCT4 transcripts in different cells. A) Our qPCR data indicated that none of OCT4 spliced variants were affected by PSORS1C3 overexpression in NT2 cells. B) In HEK293T cells, OCT4A expression level was declined 24 h post-transfection (p value=0.008) and OCT4B transcript level was upregulated (p value=0.042) since 24 hours post transfection. OCT4B1 and OCT4C were not affected by PSORS1C3 manipulation in HEK293T cells. C) PSORS1C3 over-expression dynamically affected OCT4 transcripts in HeLa cells. OCT4B level was increased 48 h after transfection (p value: 0.023). The expression level of OCT4A and OCT4C were significantly elevated (p value=0.041 and 0.02, respectively) 24 h after PSORS1C3 over-expression. OCT4B1 was not significantly affected by the manipulation.

PSORS1C3 could not cross-talk with these pathways entry, as its over-expression did not affect OCT4 expression pattern in NT2 cells.

According to its transcriptome signature, HEK293T cell line is more close to a neuroendocrine lineage which does not express high levels of stemness markers (Stepanenko and Dmitrenko, 2015). Our data indicated that overexpressing PSORS1C3 could not affect the level of OCT4B1 and C transcripts that are commonly detected in stem cells. However, ectopic expression of PSORS1C3 caused a decline in already low level of expression of OCT4A transcript at 24 hours post transfection. We also observed that 24 hours after transfection, the expression of OCT4B sored significantly and remained elevated. Previous research found that OCT4B had cytoplasmic localization and could promote cell survival in cancer cell lines, as its knock-down using RNAi led to a down-regulation in anti-apoptotic factor Bcl2 and upregulation of pro-apoptotic factor Bax (Meng et al., 2018). Moreover, OCT4B also functions in stress management pathways since it could mediate cell response to hypoxia (Lin et al., 2019) , genotoxic stress (Gao et al., 2012) and chemical shock (Cortes-Dericks et al., 2013). These findings supported the idea that OCT4B performed a homeostatic role and its functional portrait fitted our data owing to the fact that it was the only transcript variant to be altered after PSORS1C3 manipulation in a non-pluripotent non-cancerous cell line.

Former researches demonstrated that OCT4 was weakly expressed in normal cervix and its expression level gradually increased during transformation and carcinogenesis (Wang et al., 2013). In our study, over-expression of PSORS1C3 caused an up-regulation in OCT4A and C transcripts 24 after transfection. However, their expression declined to the baseline expression 24 hours later, that indicated the persistence of cells to retain their normal transcription pattern despite the manipulation. This observation might be due to a non-canonical function of OCT4 in controlling mitotic entry in HeLa cells (Zhao et al., 2014). Zhao et al. reported that ectopic expression of OCT4 could delay cell cycle progression in HeLa cells. Hence, the observed resistance in OCT4A and C expression alterations in our study could be due to the activation of other regulatory circuits that fine-tune OCT4 expression to suit the cell homeostatic needs.

Our qPCR data also indicated that OCT4B transcript was increased 48 hours after transfection of HeLa cells with PSORS1C3 expressing vectors. The fact that there was a gap between expression responses of OCT4 different transcripts (OCT4A/C and OCT4B) after manipulation supported their different roles in cells and consequently diverse regulation on their expression level. It also proposed the idea that PSORS1C3 could modulate the expression level of different OCT4 variants in a dynamic manner and in accordance with cells regulatory network and genetic background.

Majority of lncRNAs function as modulators of other genes expression or effectors in cell regulatory pathways (Schor et al., 2018). Their expressions are cell- and state- specific and although their functions are not mostly vital for cells, but affect cell viability under stressed

conditions. lncRNAs are also necessary for optimum functioning of different signaling pathways (Nakagawa, 2016; Schor et al., 2018). As a transposon-derived OCT4 overlapping lncRNA, PSORS1C3 was not expressed in stem cells but showed a relative co-expression with its entangled gene in somatic carcinoma cell lines. Our presented data implied that PSORS1C3 could affect OCT4 expression level, according to the cells molecular context. However, uncovering the exact molecular mechanism behind this observation needs further investigations.

Conflict of interests

None.

References

Arvey A., Agius P., Noble W.S. and Leslie C. (2012) Sequence and chromatin determinants of cell-type-specific transcription factor binding. Genome research 22: 1723-1734.

Asadi M.H., Mowla S.J., Fathi F., Aleyasin A., Asadzadeh J. and Atlasi Y. (2011) OCT4B1, a novel spliced variant of OCT4, is highly expressed in gastric cancer and acts as an antiapoptotic factor. International Journal of Cancer 128: 2645-2652.

Atlasi Y., Mowla S.J., Ziaee S.A. and Bahrami A.R. (2007) OCT-4, an embryonic stem cell marker, is highly expressed in bladder cancer. International Journal of Cancer 120: 1598-1602.

Atlasi Y., Mowla S.J., Ziaee S.A., Gokhale P.J. and Andrews P.W. (2008) OCT4 spliced variants are differentially expressed in human pluripotent and nonpluripotent cells. Stem Cells 26: 3068-3074.

Bai M., Yuan M., Liao H., Chen J., Xie B., Yan D., Xi X., Xu X., Zhang Z. and Feng Y. (2015) OCT4 pseudogene 5 upregulates OCT4 expression to promote proliferation by competing with miR-145 in endometrial carcinoma. Oncology reports 33: 1745-1752.

Bhat S.A., Ahmad S.M., Mumtaz P.T., Malik A.A., Dar M.A., Urwat U., Shah R.A. and Ganai N.A. (2016) Long non-coding RNAs: Mechanism of action and functional utility. Noncoding RNA Res 1: 43-50.

Campbell P.A., Perez-Iratxeta C., Andrade-Navarro M.A. and Rudnicki M.A. (2007) Oct4 targets regulatory nodes to modulate stem cell function. PLoS One 2: 553-564.

Chang Y.T., Hsu C.Y., Chou C.T., Lin M.W., Shiao Y.M., Tsai C.Y., Yu C.W., Shiue J.J., Lee Y.F., Huang C.H., Chen C.C., Lee D.D., Wang W.J., Liu H.N. and Tsai S.F. (2007) The genetic polymorphisms of POU5F1 gene are associated with psoriasis vulgaris in Chinese. J Dermatol Sci 46: 153-156.

Cortes-Dericks L., Yazd E.F., Mowla S.J., Schmid R.A. and Karoubi G. (2013) Suppression of OCT4B enhances sensitivity of lung adenocarcinoma A549 cells to cisplatin via increased apoptosis. Anticancer Res 33: 5365-5373.

Du Z., Jia D., Liu S., Wang F., Li G., Zhang Y., Cao X., Ling E.A. and Hao A. (2009) Oct4 is expressed in human gliomas and promotes colony formation in glioma cells. Glia 57: 724-733.

Engreitz J.M., Haines J.E., Perez E.M., Munson G., Chen J., Kane M., Mcdonel P.E., Guttman M. and Lander E.S. (2016) Local regulation of gene expression by lncRNA promoters, transcription and splicing. Nature 539: 452-455.

Farashahi Yazd E., Rafiee M.R., Soleimani M., Tavallaei M., Salmani M.K. and Mowla S.J. (2011) OCT4B1, a novel spliced variant of OCT4, generates a stable truncated protein with a potential role in stress response. Cancer Lett 309: 170-175.

Gao Y., Wang X., Han J., Xiao Z., Chen B., Su G. and Dai J. (2010) The novel OCT4 spliced variant OCT4B1 can generate three protein isoforms by alternative splicing into OCT4B. Journal of Genetics and Genomics 37: 461-465.

Gao Y., Wei J., Han J., Wang X., Su G., Zhao Y., Chen B., Xiao Z., Cao J. and Dai J. (2012) The novel function of OCT4B isoform-265 in genotoxic stress. Stem Cells 30: 665-672.

Holm S., Sanchez F., Carlen L., Mallbris L., Ståhle M. and O'brien K. (2005) HLA-Cw 0602 Associates More Strongly to Psoriasis in the Swedish Population than Variants of the Novel 6p21. 3 Gene PSORS1C3. Acta dermato-venereologica 85: 2-8

Kelly G.M. and Gatie M.I. (2017) Mechanisms Regulating Stemness and Differentiation in Embryonal Carcinoma Cells. Stem Cells International 2017: 20-40.

Li D., Yang Z.K., Bu J.Y., Xu C.Y., Sun H., Tang J.B., Lin P., Cheng W., Huang N., Cui R.J., Yu X.G. and Zheng X.L. (2015) OCT4B modulates OCT4A expression as ceRNA in tumor cells. Oncol Rep 33: 2622-2630.

Lin S.C., Chung C.H., Chung C.H., Kuo M.H., Hsieh C.H., Chiu Y.F., Shieh Y.S., Chou Y.T. and Wu C.W. (2019) OCT4B mediates hypoxia-induced cancer dissemination. Oncogene 38: 1093-1105.

Lin Y., Ding C., Zhang K., Ni B., Da M., Hu L., Hu Y., Xu J., Wang X., Chen Y., Mo X., Cui Y., Shen H., Sha J., Liu J. and Hu Z. (2015) Evaluation of regulatory genetic variants in POU5F1 and risk of congenital heart disease in Han Chinese. Scientific reports 5: 15860-15860.

Malakootian M., Mirzadeh Azad F., Naeli P., Pakzad M., Fouani Y., Taheri Bajgan E., Baharvand H. and Mowla S.J. (2017) Novel spliced variants of OCT4, OCT4C and OCT4C1, with distinct expression patterns and functions in pluripotent and tumor cell lines. European Journal of Cell Biology 96: 347-355

Maragkoudaki M., Vaiopoulou A., Theodoropoulos G.E., Legaki E., Sechi L.A., Karamanolis G., Zografos G. and Gazouli M. (2015) Specific detection of OCT4 isoforms in inflammatory bowel disease. Gut pathogens 7: 25-25.

Meng L., Hu H., Zhi H., Liu Y., Shi F., Zhang L., Zhou Y. and Lin A. (2018) OCT4B regulates p53 and p16 pathway genes to prevent apoptosis of breast cancer cells. Oncology letters 16: 522-528.

Murphy T.M., Crawford B., Dempster E.L., Hannon E., Burrage J., Turecki G., Kaminsky Z. and Mill J. (2017) Methylomic profiling of cortex samples from completed suicide cases implicates a role for PSORS1C3 in major depression and suicide. Transl Psychiatry 7: 989-998.

Nakagawa S. (2016) Lessons from reverse-genetic studies of lncRNAs. Biochimica et Biophysica Acta (BBA) - Gene Regulatory Mechanisms 1859: 177-183.

Rijlaarsdam M.A., Van Herk H.a.D.M., Gillis A.J.M., Stoop H., Jenster G., Martens J., Van Leenders G.J.L.H., Dinjens W., Hoogland A.M., Timmermans M. and Looijenga L.H.J. (2011) Specific detection of OCT3/4 isoform A/B/B1 expression in solid (germ cell) tumours and cell lines: confirmation of OCT3/4 specificity for germ cell tumours. British Journal Of Cancer 105:854-863.

Schor I.E., Bussotti G., Maleš M., Forneris M., Viales R.R., Enright A.J. and Furlong E.E.M. (2018) Non-coding RNA Expression, Function, and Variation during Drosophila Embryogenesis. Current Biology 28: 3547-3561.

Shi Y., Ye P. and Long X. (2017) Differential Expression Profiles of the Transcriptome in Breast Cancer Cell Lines Revealed by Next Generation Sequencing. Cellular Physiology and Biochemistry 44: 804-816.

Stepanenko A.A. and Dmitrenko V.V. (2015) HEK293 in cell biology and cancer research: phenotype, karyotype, tumorigenicity, and stress-induced genome-phenotype evolution. Gene 569: 182-190.

Wang X. and Dai J. (2010) Concise review: isoforms of OCT4 contribute to the confusing diversity in stem cell biology. Stem cells 28: 885-893.

Wang Y., Xu Z., Jiang J., Xu C., Kang J., Xiao L., Wu M., Xiong J., Guo X. and Liu H. (2013) Endogenous miRNA Sponge lincRNA-RoR Regulates Oct4, Nanog, and Sox2 in Human Embryonic Stem Cell Self-Renewal. Developmental Cell 25: 69-80.

Wang Y.D., Cai N., Wu X.L., Cao H.Z., Xie L.L. and Zheng P.S. (2013) OCT4 promotes tumorigenesis and inhibits apoptosis of cervical cancer cells by miR-125b/BAK1 pathway. Cell Death & Disease 4: 760-770.

Zhao R., Deibler R.W., Lerou P.H., Ballabeni A., Heffner G.C., Cahan P., Unternaehrer J.J., Kirschner M.W. and Daley G.Q. (2014) A nontranscriptional role for Oct4 in the regulation of mitotic entry. Proceedings of the National Academy of Sciences 111: 15768-15773.

Research Article

The Comparative Analysis of Gene Expression Profiles in Lymph Node Cells of Naturally BLV-infected and Uninfected Bovine

Fereshteh Ashrafi [1], Mohammadreza Nassiri [1,2*], Seyed Abdolrahim Rezaee [3], Ali Javadmanesh [1]

[1] *Department of Animal Science, Ferdowsi University of Mashhad, Mashhad, Iran*
[2] *Institute of Biotechnology, Ferdowsi University of Mashhad, Mashhad, Iran*
[3] *Immunology Research Center, Inflammation and Inflammatory Diseases Division, Mashhad University of Medical Sciences, Mashhad, Iran*

Received 23 August 2019 Accepted 28 September 2019

Abstract

Bovine leukemia virus (BLV) is the etiologic agent of enzootic bovine leucosis (EBL) for the bovine host. In this study to examine gene expression changes in the manifestation of the EBL malignancy, four pooled RNA samples (three RNAs in each sample) were applied for transcriptome sequencing using RNA-seq technique. Differential expression analysis was done to compare the infected bovine group with the healthy bovine group using DESeq2 package in R software. Furthermore, functional gene ontology (GO) term and KEGG pathway enrichment analysis were stablished using the DAVID online database to identify involved GO terms and pathways in the host response to BLV infection. Our results suggested that 371 up- and 72 downregulated genes were involved in EBL with statistically significant threshold log2foldchange (LFC) = 1 and false discovery rate (FDR) <0.05 that were enriched in 74 biological processes and 20 KEGG pathways. Most of identified genes were associated with cancer, especially B-cell malignancies. The glycolysis/glycogenesis metabolic process is activated in B cells that confers growth and survival advantages in tumor and dysregulated CXCL10, IL17R, BTK, CDK4 and SYK genes known as valid biomarkers to increase the proliferation of malignant cell. The outcomes can provide a list of involved genes in the malignancy and help to screen candidate genes for cancer therapy in the future.

***Keywords*:** BLV, EBL, transcriptome, RNA-Seq, Gene Ontology

Introduction

Bovine leukemia virus, a deltaretrovirus related to human T-cell leukemia virus types 1 and 2 (HTLV-1 and HTLV-2), causes a lethal lymphoma or lymphosarcoma, enzootic bovine leucosis, which has been defined as a prolonged course that often involves persistent lymphocytosis (PL) and ends in B-cell lymphoma (Burny et al., 1988; Juliarena et al., 2017). EBL happens in a small portion (< 5-10%) of infected adult bovine, while the majority of infected animals (~70%) remain asymptomatic carriers. The prevalence of BLV infection and inducing of EBL in carriers cause economic losses for the livestock industry in the worldwide (Polat et al., 2017) and this infection is as high as 25.4% in the northeast of Iran (Mousavi et al., 2014).

The BLV virus carries two single-strand RNA (ssRNA), which can be reverse transcribed into DNA and integrated into the host genome as a proviral DNA (Moratorio et al., 2013). It encodes a trans-activator protein Tax, which plays a leading role in viral replication and activates dysregulation of cellular genes including cytokines, adhesion molecules and growth factors at the initial steps of oncogenesis to affect viral spreading and disease progression (Arainga et al., 2012). Furthermore, Tax gene can transcriptionally change the expression level of cellular genes involved in the cell cycle, DNA repair and programmed cell death processes (Aida et al., 2013; Arainga et al., 2012; Kouznetsova et al., 2019) to provide the basis of cell transformation. Despite the activation of Tax protein, the expression of antisense transcripts AS1 and AS2 from 3'LTR side of provirus have pivotal roles in the maintenance of malignancy and escaping from host immune responses, mainly at the latent stage of malignancy (Durkin et al., 2016).

The viral infection and tax-responsive genes might not be unique supplier for the cell transformation while other additional events are required such as gene polymorphisms, chromosomal aberrations, genome instability and accumulation of mutations in cellular DNA (Klener et al., 2006) for progression of this multistep tumor in the bovine host. The existence of polymorphism in the enhancer region of TNF-α (Konnai et al., 2006) and mutation in

* Corresponding author's E-mail: *nassiryr@um.ac.ir*

oncogenes such as *P53* (Dequiedt et al., 1995) is confirmed to contribute in the progression of BLV-induced lymphoma. Therefore, the virus-host interaction manner apart from viral factors would have a principal role to induce malignancy.

The objective of this study was to investigate the gene expression changes in the host-virus interaction manner using RNA-seq technique. It is known a little about the transcriptional changes associated with abnormal B-cell growth in EBL malignancy. We compared gene expression profiles of EBL and the healthy bovine groups to identify differentially expressed genes (DEGs). Subsequently, the identified DEGs were enriched to determine functional GO terms and KEGG pathways that participate in the B-cell transformation and EBL oncogenicity.

Materials and Methods

Sample collection and EBL diagnostics

This study was approved and supervised by the ethics committee of Ferdowsi University of Mashhad, Mashhad, Iran (No. 42333). Six infected lymphoid tumors at the acute stage of the EBL disease, and six healthy lymph nodes without BLV viral infection collected from cows (3.5-4 years old), at the slaughterhouse of Mashhad, Iran, and immediately transferred to a liquid nitrogen tank. At first, the EBL disease approved by two veterinarians based on the existence of clinical symptoms. Then, a qualitative method was optimized using the *Pol* gene expression in Rotor-gene 6000 (Qiagen, Germany) machine. Reaction ingredients were composed of 10 µl commercial Real-time master mix (Thermo Fisher, USA), 0.5 µl of primers (Fw, 5'-CCTCAATTCCCTTTAAACTA-3'; Rv, 5'-GTACCGGGAAGACTGGATTA-3'), 1 µL of TaqMan probe (FAM-GAACGCCTCCAGGCCCTTCA-BHQ1) (Rola-Łuszczak et al., 2013), 2.5 µl of deionized water and 5 µl of template DNA. DNAs were extracted with high quality by using the High Pure PCR template Kit (Qiagen, Germany), according to the manufacturer's instruction.

RNA extraction and sequencing

Total RNAs were isolated using the RNeasy Mini Kit (Qiagen, Germany), according to the manufacturer's instructions. The pooled RNAs per group (infected and uninfected) were prepared by mixing equal concentrations of three biological replicates (RNAs) to generate four pooled RNA samples. The single-strand DNA (ssDNA) templates were synthesized using oligo-dT primers and reverse transcriptase, according to the manufacturer's instructions (Thermo Fisher, USA). The purity, integrity and quantity of RNAs and cDNAs with amplification of the GAPDH gene (as a reference gene) were examined on 1.5% agarose gel and NanoDrop device. The type of poly-A capturing library was used for sequencing with Illumina HiSeq 4000 platform to generate 2-100 bp paired-end reads, and 2-30 million raw paired-end read files, by the BGI Company.

Differential expression analysis

Raw reads were preprocessed using FastQC (Andrews, 2016) and Trimmomatic (Bolger et al., 2014) software; then clean reads were acquired for subsequent analyses. The clean raw paired-end read profiles from each sample were mapped to the host-provirus reference genome individually, using STAR software (v2.5.4) (Dobin et al., 2013). Host-provirus reference genome was built by merging bovine reference genome UMD3.1 with proviral genome sequence BLV-YR2 (GenBank: KT122858) before alignment. Sorting and indexing of STAR outputs were performed by SAMtools software (v1.9) (Li et al., 2009). Annotation of GTF files (v74) for bovine, was downloaded from Ensemble database, and custom BLV virus annotation was built by HTLV-1/BLV genomics lab in Medical Genomics/Unit of Animal Genomics (UAG), Liege, Belgium. The FeacureCounts package was used for reads quantification (Liao et al., 2013). Finally, differential expression analysis was performed based on statistically significant FDR $\leq$ 0.05 in R software (v.3.5), using DESeq2 package (v.1.20) (Love et al., 2014).

Gene ontology (GO) and pathway analysis

Gene ontology analysis was performed on the list of significant (DEGs) based on biological process (BP), molecular function (MF), cellular component (CC) terms and the KEGG (The Kyoto Encyclopedia of Genes and Genomes) pathway, using DAVID 6.8 web tools (https://david.ncifcrf.gov/) (Huang et al., 2009). For identification of related GO terms to our samples, the GO profiles of significant DEGs were compared to the GO profile of bovine genome annotation as a reference set. The FDR $\leq$ 0.05 and P-value $\leq$ 0.01 were considered as a cutoff threshold for statistical significance in detection of GO terms and the KEGG pathways, respectively. The identified GO terms were classified using CateGOrizer "GO term classification counter" online tools based on GO slim method (Hu et al., 2008).

Results

EBL diagnostics

The Enzootic bovine leucosis can be characterized by developing tumor masses, tumor masses which are composed of monomorphic lymphocytic cells, and variable clinical signs including cardiac lymphosarcoma, enlarged lymph nodes and discrete nodular masses or a diffuse tissue infiltrate in EBL samples that were shown in Figure 1. The amplification of *Pol* gene by real-time PCR technique confirmed the infection of EBL samples, while the healthy subjects were not seropositive for BLV infection (Figure 2).

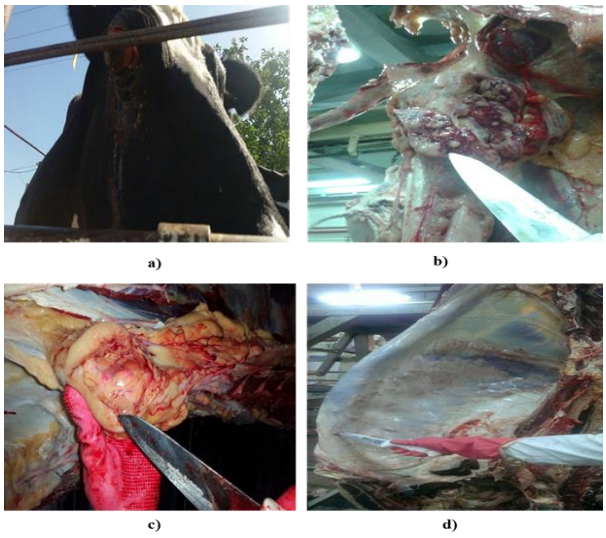

Figure 1. The clinical signs of EBL samples. a) Retro-ocular lymph node b) Cardiac lymphosarcoma, c) Enlarged mediastinal lymph node and d) Nodular masses.

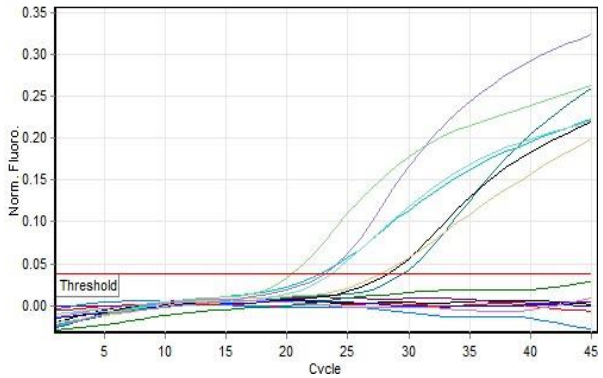

Figure 2. RT-qPCR amplification curves of *Pol* gene in healthy and infected samples.

RNA extraction and preprocessing of raw reads

The appearance of 28S and 18S ribosomal RNA and amplification of GAPDH gene as a reference on a 1.5% agarose gel, had proven the quality of RNA and cDNA products (Figure 3). Pooled samples (2 samples per group) were sequenced based on high throughput sequencing and by using of Illumia Hiseq 4000 platform. Almost 2-30 million paired-end raw read profiles were obtained per sample from the company. All reads passed the preprocessing cutoff thresholds using FastQC software and only the adaptor contaminations were trimmed off by using Trimmomatic software.

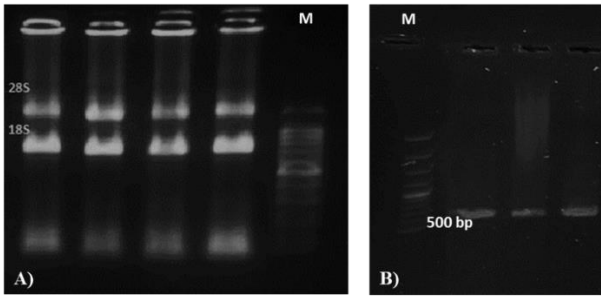

Figure 3. The integrity of RNA and complementary DNA amplification (cDNA)**.** A) The RNA quality of samples based on 28S and 18S ribosomal RNA. B) cDNA quality with amplification of the *GAPDH* gene. Lane M shows 100 bp plus DNA marker.

Differential expression analysis

Read mapping was carried out using STAR aligner, a splice junction aware software. Most of the reads (60.7-79.5%) were mapped to the reference genome. The result of the DE analysis suggested 443 unique genes that were differentially expressed in the infected group, compared to the healthy group. The identification of significant genes was based on the FDR ≤0.05. Around 371 genes were over-expressed with positive Log2–fold change more than 2, and 72 genes were under-expressed with negative Log2 fold change less than 2, in infected samples versus control samples. The detailed information of the discovered genes is presented in Supplementary data file sheet1.

Functional GO terms and pathway analysis

The Gene Ontology enrichment analysis was accomplished for better understanding of the biological processes and involved pathways of identified DEGs in EBL malignancy. There were 112 significant improved GO terms based on FDR ≤ 0.05 (30, 8 and 74 for CC, MF and BP categories, respectively) (see supplementary data file sheet 2). Because of redundancy and overlapping among identified GO term results, they were classified using GO slim method in CateGOrizer online tool to describe the basic terms and relationships between terms within the context of biology (Table 1). A term

Table 1. The classified Gene Ontology (GO) terms of DEGs, using CateGOrizer online tool.

Parent GO ID	GO Definitions	GO terms	Counts	Fractions
GO:0008150	biological-process	BP	74	36.63%
GO:0008152	metabolism	BP	64	14.36%
GO:0009058	biosynthesis	BP	29	11.39%
GO:0006139	nucleobase, nucleoside, nucleotide and nucleic acid metabolism	BP	23	1.49%
GO:0016043	cell organization and biogenesis	BP	3	1.49%
GO:0006259	DNA metabolism	BP	3	0.99%
GO:0006996	organelle organization and biogenesis	BP	2	0.99%
GO:0007049	cell cycle	BP	2	0.50%
GO:0007165	signal transduction	BP	1	0.50%
GO:0007154	cell communication	BP	1	14.36%
GO:0005575	cellular_component	CC	29	41.43%
GO:0005623	cell	CC	16	22.86%
GO:0005622	intracellular	CC	13	18.57%
GO:0005576	extracellular region	CC	5	7.14%
GO:0005634	nucleus	CC	4	5.71%
GO:0005856	cytoskeleton	CC	1	1.43%
GO:0005737	cytoplasm	CC	1	1.43%
GO:0005730	nucleolus	CC	1	1.43%
GO:0003674	molecular_function	MF	8	36.36%
GO:0005488	binding	MF	8	36.36%
GO:0003676	nucleic acid binding	MF	3	13.64%
GO:0003723	RNA binding	MF	2	9.09%
GO:0000166	nucleotide binding	MF	1	4.55%

Only the basic (parent) GO terms are presented. BP, biological process; CC, cellular component; MF, molecular function; Counts are the number of identified GO terms in each class term; Fractions are the percentage of identified GO terms that grouped in each class term.

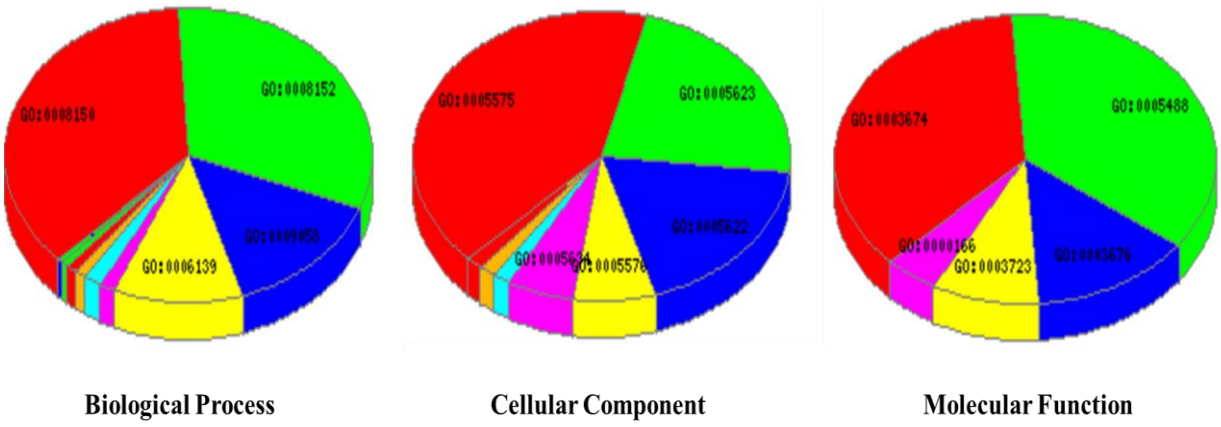

Figure 4. The classified basic Gene Ontology (GO) terms in pie graphs.

may classify in a subset of different terms. The presented percentage in the fraction column of Table 1, express the importance of the identified basic (parent) terms that consisted of child terms. The two top basic terms were metabolism and biosynthesis in BP category, cell and intracellular in CC category, binding and nucleic acid binding in MF category (Figure 4). Our result suggested 20 significant KEGG pathways based on statistically significant *P*-value ≤ 0.01 (Dahiru, 2008) (Table 2). The five top significant KEGG pathways were PI3K-Akt signaling pathway, pathway in cancer, biosynthesis of antibiotics, proteoglycans in cancer, cardiac muscle contraction and B cell receptor (BCR) signaling pathway, in EBL group.

Table 2. The enriched KEGG pathways of DEGs by using DAVID online tool

KEGG ID	Pathway	Counts	%	Pop hits	P-value
bta04151	PI3K-Akt signaling pathway	28	6.378	347	1.33E-05
bta05200	Pathways in cancer	30	6.833	398	2.18E-05
bta01130	Biosynthesis of antibiotics	20	4.555	206	2.74E-05
bta05205	Proteoglycans in cancer	19	4.328	203	7.49E-05
bta04260	Cardiac muscle contraction	11	2.505	80	2.04E-04
bta04662	B cell receptor signaling pathway	10	2.277	70	3.42E-04
bta04916	Melanogenesis	11	2.505	99	0.001
bta04310	Wnt signaling pathway	13	2.961	137	0.001
bta05166	HTLV-I infection	19	4.328	267	0.002
bta04912	GnRH signaling pathway	9	2.050	86	0.005
bta04512	ECM-receptor interaction	9	2.050	87	0.006
bta04020	Calcium signaling pathway	14	3.189	189	0.007
bta05217	Basal cell carcinoma	7	1.594	55	0.007
bta05219	Bladder cancer	6	1.366	40	0.008
bta04915	Estrogen signaling pathway	9	2.050	98	0.01
bta00010	Glycolysis / Gluconeogenesis	7	1.594	63	0.01
bta04510	Focal adhesion	14	3.189	208	0.01
bta04660	T cell receptor signaling pathway	9	2.05	105	0.01
bta05414	Dilated cardiomyopathy	8	1.82	86	0.01
bta04611	Platelet activation	10	2.27	127	0.01

Only the significantly enriched KEGG pathways ($P \leq 0.01$) are presented. Counts are the number of unique DAVID gene symbol corresponding to our input gene list; Pop hits, the number of genes that belong to the specific gene category.

Discussion

The development and progression of leukemogenesis induced by BLV, depend on the level of viral factors such as *Tax* gene expression at the early stage of infection, while some recent studies have been reported that besides of infection, the immune deterioration, growth factor production and activation of cancer driver genes can induce cell transformation and malignancy to form acute phase of infection (Durkin et al., 2016; Gillet et al., 2007). Hence, the study of bovine's transcriptome at the acute phase is helpful for a better understanding of involved genes and pathways in the manifestation of the EBL.

In this study, we produced high throughput transcriptome data using RNA-seq technique from 4 pooled RNA samples to examine gene expression changes in lymph node cells of two EBL samples in the counterpart of two sera-negative samples in response to BLV infection and progression to the lymphocytic stage. The expression of 443 unique DEGs was changed through BLV infection, 371 were up- and 72 were downregulated. Of note, previous studies were applied microarray technique (Brym and Kamiński, 2017; Everts et al., 2005; Klener et al., 2006) for investigation of gene expression changes, while we used RNA-seq technique for the first time. There are only a few DEGs in common between our result and the DEG lists of some microarray studies (e.g *ADORA2B*, *CD19*, *APEX1*, *HIF1A*, *CCT5*, *LMO2*, *HADH*, *DYNLL1*, *C1QBP*, *BCL11A*, *SYK*, *PHGDH*, *WDFY4*, *NMI*, *CXXC5*, *SOX5*, *CYB5R3*, *RHNO1*, *YWHAG*, *LYN*, *Src*, *PEBP1*, *GNL3*, *CXXC5*, *ERH*, *AVEN*, *CMTM7*, *NACA*, *HSPA14*, *ENOPH1*, *LCN2*, *HMGB1*, *CXCL10*, *DYNLL1*, *CXHXorf57*, *ZBTB32*, *TUBB4B*, and *PKM*) and a few DEGs with invert expression (e.g. *HSPA4*, *IL17R*, *CDK4*, *RNASE6*, *SDCBP*, *GAPDH*, *RGS2*, *MKI67*, *TOP2A*, and *CD79A*) (Brym and Kamiński, 2017; Everts et al., 2005; Klener et al., 2006). It is interesting that genes associated with several human malignancies, especially B-cell tumor, were represented among the differentially expressed genes. Some genes were

new and had no recognized role in tumor development.

The upregulated *CXCL10* was significantly associated with tumor cell migration and progression in diffuse large B-cell lymphoma (DLBCL) (Burny et al., 1988) and is a valid biomarker in progress of heart failure (Greenwood et al., 2018). In the EBL samples, the pathway of cardiac muscle contraction was significant, and heart failure might be a sign of clinical symptom of EBL malignancy. The upregulation of *TOP2A* and *MKI67* in prostate cancer (Malhotra et al., 2011) and *CDK4* in B cell lymphoma (Brym and Kamiński, 2017) are resulted to increase the proliferation of malignant cell and they might be good candidates for targeted cancer therapy.

B cells are the main arm of humoral immunity, which is targeted by BLV, thus BCR and three membranes of B cell antigen receptors complex, *CD79A*, *CD19*, and *CD70A*, as most pivotal activators were upregulated in infected BLV cells (Brym and Kamiński, 2017). This strategy of BLV for B cell survival via BCR signaling (Burny et al., 1988) is the homolog of the activation of TCR signaling in HTLV-1 infection (Ghezeldasht et al., 2013) to induce cell cycle promoting proteins, provides growth factors in cell survival to inhibit apoptosis, and activates transforming pathways for malignancy. Activation of the BCR complex leads to the phosphorylation of proto-oncogenes tyrosine kinases family, including *BTK* and SYK in hematopoietic cells (Gauld and Cambier, 2004). High expression of *BTK* and *SYK* genes increase the activation, proliferation, and survival of DLBCL (Gauld and Cambier, 2004; Tolar et al., 2005).

Further, the identified differentially expressed genes were used in the gene enrichment analysis by using the online DAVID database to screen functional patterns associated with the expression differences observed. In general, our result suggested 74 BP, 30 CC and 8 MF. Because of the existence of more similarity and redundancy among obtained Go terms, we categorized GO terms in terms of basic GO classes using CateGorizer online tool based on GO slim method to reveal the main basic 'parent' GO terms and the relationships between 'child' terms (Hu et al., 2008). Finally, whole expressed genes were localized in 7 cellular component term including cell, intracellular or extracellular region, nucleus, cytoskeleton, cytoplasm and nucleus; and were involved in 9 biological processes including metabolism; biosynthesis; nucleobase, nucleoside, nucleotide and nucleic acid metabolism; cell organization and biogenesis; DNA metabolism; organelle organization and biogenesis; cell cycle; signal transduction and cell communication which they mediated four molecular functions including binding; nucleic acid binding; RNA binding and nucleotide-binding. These enrichment results provided further supports to previously published results about the invasion of BLV infected cells (Brym and Kamiński, 2017; Everts et al., 2005; van den Heuvel et al., 2005).

Furthermore, our study suggests the expression changes in genes from 20 distinct KEGG pathways, including PI3K-Akt signaling pathway; pathway in cancer; biosynthesis of antibiotics; proteoglycans in cancer; cardiac muscle contraction; B cell receptor signaling pathway; melanogenesis; Wnt signaling pathway; HTLV-1 infection; GnRH signaling pathway; ECM-receptor interaction; calcium signaling pathway; Basal cell carcinoma; Bladder cancer; estrogen signaling pathway; glycolysis/gluconeogenesis; focal adhesion; T-cell receptor signaling pathway; dilated cardiomyopathy and platelet activation. The dysregulation and activation of mentioned KEGG pathways, leading to the disruption of B-cell survival and growth control. Interestingly, these activated processes were reported previously with HTLV-1, a T-cell-tropic oncoretrovirus, as well as non-virus-associated human B-cell malignancies (Liu et al., 2018; Mozhgani et al., 2018).

The activation of cellular adhesion molecules (CAMs) and focal adhesion process play central roles in transferring and localization of leukemic cells in different tissues that finally affect cancer cell growth and metastasis (Brym and Kamiński, 2017; Burny et al., 1988). More studies are needed to explain the impact of the adhesion process in BLV infiltration to host cells. The glycolysis/gluconeogenesis pathway happens inside the cells to produce adenosine triphosphate (ATP), as a cell energy, to drive many processes in cells. Recent studies have reported the high activation of glycolysis/gluconeogenesis, PI3K-AKT signaling pathway, B cell and T cell receptor signaling pathway in cancer cells, including colorectal cancer, adult T cell leukemia (ATLL), and diffuse large B cell lymphoma (DLBCL) compared to normal cells (Caro et al., 2012; Liu et al., 2018; Mozhgani et al., 2018). Our results indicated that the glycolysis metabolic process was activated in B cells that confers growth and survival advantages in the tumor.

In conclusion, a wide range of effective, up- and downregulated genes involved in EBL pathogenicity and malignancy were introduced by the present study. More identified processes including ECM-

receptor interaction, focal adhesion, BCR signaling, TCR signaling, glycolysis/gluconeogenesis, PI3K-Akt pathway and the dysregulated genes including *CXCL10*, *BTK*, *SYK*, *IL17R* and *CDK4* were associated with the disruption of natural DNA replication and cell proliferation which induce the repression of DNA damage responses and apoptosis in B-cells to make malignancy. Moreover, the over-activation of glycolysis/gluconeogenesis pathway along with immune cells is required to support the metabolic reprogramming of B cells. As regards EBL malignancy is a life-threatening disease for farm animals, more researches on transcriptome level are necessary to accelerate our findings of the EBL diseases.

Acknowledgments

This study was funded by Ferdowsi University of Mashhad, grant # 3/42333. We are grateful to Dr. Pooyan Amiri for his contribution to collecting samples.

Conflict of interest

All authors report no conflict of interest.

References

Aida Y., Murakami H., Takagashi M. and Takeshima S.-N. (2013) Mechanisms of pathogenesis induced by bovine leukemia virus as a model for human T-cell leukemia virus. Frontiers in microbiology 4:328.

Andrews S. (2016) FASTQC: A quality control tool for high throughput sequence data. Available from http//www.bioinformatics.babraham.ac.uk/projects/fastqc.

Arainga M., Takeda E. and Aida Y. (2012) Identification of bovine leukemia virus tax function associated with host cell transcription, signaling, stress response and immune response pathway by microarray-based gene expression analysis. BMC genomics 13:121.

Bolger A. M., Lohse M. and Usadel B. (2014) Trimmomatic: a flexible trimmer for Illumina sequence data. Bioinformatics 30:2114-2120.

Brym P. and Kamiński S. (2017) Microarray analysis of differential gene expression profiles in blood cells of naturally BLV-infected and uninfected Holstein–Friesian cows. Molecular biology reports 44:109-127.

Burny A., Cleuter Y., Kettmann R., Mammerickx M., Marbaix G., Portetelle D., Van den Broeke A., Willems L. and Thomas R. 1988. Bovine leukaemia: facts and hypotheses derived from the study of an infectious cancer. *In* Virus Infections and the Developing Nervous System. Springer. 37-56.

Caro P., Kishan A. U., Norberg E., Stanley I. A., Chapuy B., Ficarro S. B., Polak K., Tondera D., Gounarides J. and Yin H. (2012) Metabolic signatures uncover distinct targets in molecular subsets of diffuse large B cell lymphoma. Cancer cell 22:547-560.

Dahiru T. (2008) P-value, a true test of statistical significance? A cautionary note. Annals of Ibadan postgraduate medicine 6:21-26.

Dequiedt F., Kettmann R., Burny A. and Willems L. (1995) Mutations in the p53 tumor-suppressor gene are frequently associated with bovine leukemia virus-induced leukemogenesis in cattle but not in sheep. Virology 209:676-683.

Dobin A., Davis C. A., Schlesinger F., Drenkow J., Zaleski C., Jha S., Batut P., Chaisson M. and Gingeras T. R. (2013) STAR: ultrafast universal RNA-seq aligner. Bioinformatics 29:15-21.

Durkin K., Rosewick N., Artesi M., Hahaut V., Griebel P., Arsic N., Burny A., Georges M. and Van den Broeke A. (2016) Characterization of novel Bovine Leukemia Virus (BLV) antisense transcripts by deep sequencing reveals constitutive expression in tumors and transcriptional interaction with viral microRNAs. Retrovirology 13:33.

Everts R. E., Band M. R., Liu Z. L., Kumar C. G., Liu L., Loor J. J., Oliveira R. and Lewin H. A. (2005) A 7872 cDNA microarray and its use in bovine functional genomics. Veterinary immunology and immunopathology 105:235-245.

Gauld S. B. and Cambier J. C. (2004) Src-family kinases in B-cell development and signaling. Oncogene 23:8001.

Ghezeldasht S. A., Shirdel A., Assarehzadegan M. A., Hassannia T., Rahimi H., Miri R. and Rezaee S. R. (2013) Human T lymphotropic virus type I (HTLV-I) oncogenesis: molecular aspects of virus and host interactions in pathogenesis of adult T cell leukemia/lymphoma (ATL). Iranian journal of basic medical sciences 16:179.

Gillet N., Florins A., Boxus M., Burteau C., Nigro A., Vandermeers F., Balon H., Bouzar A.-B., Defoiche J. and Burny A. (2007) Mechanisms of

leukemogenesis induced by bovine leukemia virus: prospects for novel anti-retroviral therapies in human. Retrovirology 4:18.

Greenwood A. D., Ishida Y., O'Brien S. P., Roca A. L. and Eiden M. V. (2018) Transmission, evolution, and endogenization: lessons learned from recent retroviral invasions. Microbiology and molecular biology reviews 82:e00044-00017.

Hu Z.-L., Bao J. and Reecy J. M. (2008) CateGOrizer: a web-based program to batch analyze gene on-tology classification categories. Online journal of bioinformatics 9:108-112.

Huang D. W., Sherman B. T. and Lempicki R. A. (2009) Systematic and integrative analysis of large gene lists using DAVID bioinformatics resources. Nature protocols 4:44.

Juliarena M. A., Barrios C. N., Lützelschwab C. M., Esteban E. N. and Gutiérrez S. E. (2017) Bovine leukemia virus: current perspectives. Virus adaptation and treatment 9:13-26.

Klener P., Szynal M., Cleuter Y., Merimi M., Duvillier H., Lallemand F., Bagnis C., Griebel P., Sotiriou C. and Burny A. (2006) Insights into gene expression changes impacting B-cell transformation: cross-species microarray analysis of bovine leukemia virus tax-responsive genes in ovine B cells. Journal of virology 80:1922-1938.

Konnai S., Usui T., Ikeda M., Kohara J., Hirata T.-i., Okada K., Ohashi K. and Onuma M. (2006) Tumor necrosis factor-alpha genetic polymorphism may contribute to progression of bovine leukemia virus-infection. Microbes and infection 8:2163-2171.

Kouznetsova V., Chen S. and Tsigelny I. (2019) HTLV-1 can be involved in acceleration of different nonhematological cancers. Journal of cancer research and therapeutics 7:1-8.

Li H., Handsaker B., Wysoker A., Fennell T., Ruan J., Homer N., Marth G., Abecasis G. and Durbin R. (2009) The sequence alignment/map format and SAMtools. Bioinformatics 25:2078-2079.

Liao Y., Smyth G. K. and Shi W. (2013) featureCounts: an efficient general purpose program for assigning sequence reads to genomic features. Bioinformatics 30:923-930.

Liu Z., Meng J., Li X., Zhu F., Liu T., Wu G. and Zhang L. (2018) Identification of hub genes and key pathways associated with two subtypes of diffuse large B-cell lymphoma based on gene expression profiling via integrated bioinformatics. BioMed research international 2018.

Love M. I., Huber W. and Anders S. (2014) Moderated estimation of fold change and dispersion for RNA-seq data with DESeq2. Genome biology 15:550.

Malhotra S., Lapointe J., Salari K., Higgins J. P., Ferrari M., Montgomery K., van de Rijn M., Brooks J. D. and Pollack J. R. (2011) A tri-marker proliferation index predicts biochemical recurrence after surgery for prostate cancer. PLoS One 6:e20293.

Moratorio G., Fischer S., Bianchi S., Tomé L., Rama G., Obal G., Carrión F., Pritsch O. and Cristina J. (2013) A detailed molecular analysis of complete bovine leukemia virus genomes isolated from B-cell lymphosarcomas. Veterinary research 44:19.

Mousavi S., Haghparast A., Mohammadi G. and Tabatabaeizadeh S.-E. 2014. Prevalence of bovine leukemia virus (BLV) infection in the northeast of Iran. *In* Veterinary research forum: an international quarterly journal. Vol. 5. Faculty of Veterinary Medicine, Urmia University, Urmia, Iran. 135.

Mozhgani S. H., Zarei-Ghobadi M., Teymoori-Rad M., Mokhtari-Azad T., Mirzaie M., Sheikhi M., Jazayeri S. M., Shahbahrami R., Ghourchian H. and Jafari M. (2018) Human T-lymphotropic virus 1 (HTLV-1) pathogenesis: A systems virology study. Journal of cellular biochemistry 119:3968-3979.

Polat M., Takeshima S.-n. and Aida Y. (2017) Epidemiology and genetic diversity of bovine leukemia virus. Virology journal 14:209.

Rola-Łuszczak M., Finnegan C., Olech M., Choudhury B. and Kuźmak J. (2013) Development of an improved real time PCR for the detection of bovine leukaemia provirus nucleic acid and its use in the clarification of inconclusive serological test results. Journal of virological methods 189:258-264.

Tolar P., Sohn H. W. and Pierce S. K. (2005) The initiation of antigen-induced B cell antigen receptor signaling viewed in living cells by fluorescence resonance energy transfer. Nature immunology 6:1168.

Van den Heuvel M. J., Jefferson B. J. and Jacobs R. M. (2005) Purified bovine plasma blocking factor decreases Bovine leukemia virus p24 expression while increasing protein synthesis and transcriptional activity of peripheral blood

mononuclear cells in short-term culture. Canadian journal of veterinary research 69:186.

Research Article

The LEPR (853A>G and 511A>G) Transitions may Enhance Idiopathic Recurrent Miscarriage: Evidences Based on Case-control and *in silico* Studies

Abasalt Hosseinzadeh Colagar*, Masomeh Salehi-Doon

Department of Molecular and Cell Biology, Faculty of Basic Sciences, University of Mazandaran, Babolsar, Iran

Received 7 July 2019 Accepted 3 August 2019

Abstract

Previous studies in human leptin receptor protein (LEPR) signaling are important in the establishment of fetal growth. Idiopathic recurrent miscarriage (IRM) may be the result of abnormal placental and fetal development. Thus single nucleotide polymorphisms (SNPs) of LEPR might be associated with IRM. In our case-control study, which conducted from 2017 to 2018 at the Milad Sari Genetic Detection Center and Razi Hospital (Ghaemshahr, Iran), 140 samples, including 70 cases with history of three or more IRM as before the 22nd week of gestation, and 70 controls with at least two live births and no history of pathologic pregnancies during reproductive period were studied. Polymorphisms of maternal LEPR 853A>G and 511A>G were assessed by PCR-RFLP and SSCP, respectively. Results showed that 853A>G SNP, contained frequent genotype AG (p= 0.002; OR= 0.391; 95% CI= 0.154-0.664) and G allele (p= 0.003; OR= 0.125; 95% CI= 0.032–0.489), revealed a significant protective association with IRM. Primary screening of 511A>G showed that 63 case-samples were AG genotype. PCR directed sequence showed this SNP contained frequent genotype for AG (p= 0.001; OR= 0.57; 95% CI= 0.22-0.147) and G allele (p= 0.006; OR= 0.34; 95% CI= 0.008–0.149), revealed a significant protective association with IRM. Based on our findings, LEPR (853A>G and 511A>G) gene transitions not only might enhance IRM but also could be useful genetic markers in susceptibility and severity of recurrent miscarriage.

***Keywords*:** LEPR gene, obesity, recurrent miscarriage

Introduction

Idiopathic recurrent miscarriage is a common problem that affects 10 to 15% of known clinical pregnancies (Yan et al., 2012). It has been reported that 0.5 to 1% of couples suffer from idiopathic recurrent miscarriage, and in 40 to 50% of them, the reason is unknown (Chin et al., 2013). Idiopathic recurrent miscarriage (IRM) or idiopathic recurrent spontaneous abortion (IRSA) is determined as the loss of gestation before 20 weeks (Matthiesen et al., 2012), that defined by two or three continuous miscarriage (Kolte et al., 2015; Silver et al., 2011). The factors involved can be referred to infections (Nigro et al., 2011), antiphospholipid syndromes (Da et al., 2017), maternal disease (Yang et al., 2017), thrombophilias (Kar et al., 2017), genetic disorder (AlShaikh et al., 2011). Some of the genes involved in miscarriage including: Zpi (Pang et al., 2013), Vegf (Messaoudi et al., 2013), Stat3 (Su et al., 2011), Progen (Shin et al., 2013), Nos3 (Fraga et al., 2014), P53 (Shahsavari et al., 2015), Kdr (Muller et al., 2013), and LEPR (Dias et al., 2012). The leptin receptor protein (LEPR), which known as OB-R, and CD295 (Baumann et al., 1996), is located on the choromosom1p31.3 with 24 exons (Bartha et al., 2005). Leptins, which secreted by the adipose tissue, attached to the receptors which are located in the hypothalamus and follicular-ovarian cells. These peptide hormones regulate homeostasis of energy (Considine et al., 1996). The LEPR protein categorized as interleukin-6 from the family of type 1 cytokines with six isoforms: LEPR-a, b, c, d, e, and f (Zhou et al., 2015). Isoforms of LEPR-a, c, d, and f are short but LEPR-b isoform is long. The LEPR gene involves in some diseases including: type2 diabetes mellitus (Wang et al., 2017), breast cancer (Cleveland et al., 2010), prostate cancer (Alshaker et al., 2015), lung cancer (Unsal et al., 2014) and idiopathic recurrent miscarriage (Muller et al., 2016). Previous studies have reported that the role of LEPR in idiopathic recurrent miscarriage could vary among different populations. Expression of LEPR-b and LEPR-a are effective in stimulation of LH in the rat ovaries (Ramirez et al., 2017). Leptin receptor has been known in the vascular endothelial cells of a fetal vessel of chorionic villi during the early pregnancy (Muhlhauser et al., 1996). Researchers have also suggested that single nucleotide polymorphisms (SNPs) of the LEPR 853A>G (as

*Corresponding author's E-mails: acolagar@yahoo.com; ahcolagar@umz.ac.ir

Table 1. Oligomers used as primers and PCR conditions.

SNP	Primers Names	Oligomers (5'→ 3')	Cycles and thermal conditions	PCR product
853A>G (rs1137101)	*LEPR1-f*	5'-TCCTGCTTTAAAAGCCTATCC	35 cycles of 94°C for 5 min, 94°C for 30s, 58°C for 30s, and 72°C for 30s; final extension at 72°C for 5 min	417 bp
	LEPR1-r	5'-GTAGATGTAGTACTGGGGGTA		
511A>G (rs1137100)	*LEPR2-f*	5'- CTTTTGCCTGCTGGACTCTC	35 cycles of 94°C for 5 min, 94°C for 30s, 58°C for 30s, and 72°C for 30s; final extension at 72°C for 5 min	217 bp
	LEPR2-r	5'- AAACTAAAGAATTTACTGTTGAAACAAATGTC		

known: Gln223Arg; A177266G; 853Q>R; rs1137101) in the exon 7 (Figure 1A) and LEPR 511A>G (as known as: Lys109Arg; A155194G; 511A>G; rs1137100) in exon 5 (Figure 1A) can be related to idiopathic recurrent miscarriage (Muller et al., 2016; Riestra et al., 2011). SNPs in the translation process can cause different structural changes in the mRNA (Ng and Henikoff et al., 2006). The nonsynonymous single nucleotide polymorphism (nsSNP) is as a gene variation which can affect in the structure and stability, ligand binding specifications, catalysis and post-translational modification (PTM), protein-protein interaction (PPI) and hydrophobicity content of proteins (Aftabi et al., 2016; David et al., 2012). In biomedical sciences, the current significance and effectiveness of bioinformatics and silica tools have recently been studied (Mehmood et al., 2014; Chou et al., 2015). In the present study, the association of 853A>G and 511A>G with idiopathic recurrent miscarriage and *in silico* analysis were investigated.

Materials and Methods

Blood sample collection

In a case-control trial for a total of 140 women, citrate blood samples were collected from 70 cases with 20-45 years old, with history of ≥ 3 successive miscarriages; and 70 controls, with 19-50 years old, with history of ≥ 3 successful gestations. In the case group, patients with a known cause of pregnancy loss (chromosomal impairment, chronic disease, infection, hormonal defect, antiphospholipid antibodies, thromboembolic disease, cervical inadequacy, or other obstetric complications that could cause abortion fetus (such as hypertension, preeclampsia, eclampsia, gestational diabetes mellitus) were excluded (Ramirez et al., 2017). In the control group, all women with a history of abortion fetus, thrombotic changes associated with other obstetric complications, preterm placental ablation, intrauterine fetal death, and chronic diseases were also excluded (Ramirez et al., 2017). All participants were from Milad Sari Genetic Detection Center and Razi Hospital (Ghaemshahr, Iran), between 2016 up to Aug. 2018. These study approved by the ethics committees of the University of Mazandaran (#IR.UMZ.REC.1397.028) and informed consent was obtained from each subject before participation.

Amplification of SNPs flanking fragments

The genomic DNA was isolated from all blood samples by a commercial DNA extraction kit (Cinnagen Co, Iran). For amplification of LEPR-SNPs flanking fragments, 4 oligomers were designed by Oligo7 software and fragments amplified by PCR program at Mastercycler EP Gradient thermal cycler conditions (Table 1). All of the PCR reactions were performed at a final volume of 25 µl, which consisted of 10 pM of each primer, 0.75 mM of MgCl2, 0.2 mM of mix-dNTPs and 0.06 U of *Taq* DNA polymerase.

PCR-RFLP and SNP genotyping

LEPR 853A>G polymorphism was analyzed by polymerase chain reaction-restriction fragment length polymorphism (PCR-RFLP) method using primers and restriction enzyme. 2.5 µl of PCR products digested with 0.3 U of *Msp*I restriction enzyme (Fermentas Co, Germany) and 1X buffer at 37 °C for 16 h. Digested fragments electrophoresed in 1.5% agarose gel and stained by 1µg/ml ethidium bromide stock solution. Agarose gel electrophoresis and gel staining were performed through Green and Sambrook (2012) methods. At least three PCR direct-sequences products were evaluated (Takapouzist Co., Iran) for verification of PCR-RFLP results.

Statistical analysis

For various alleles and genotypes in case and control groups, odds ratio (OR) with 95% confidence interval (95% CI) was calculated. The

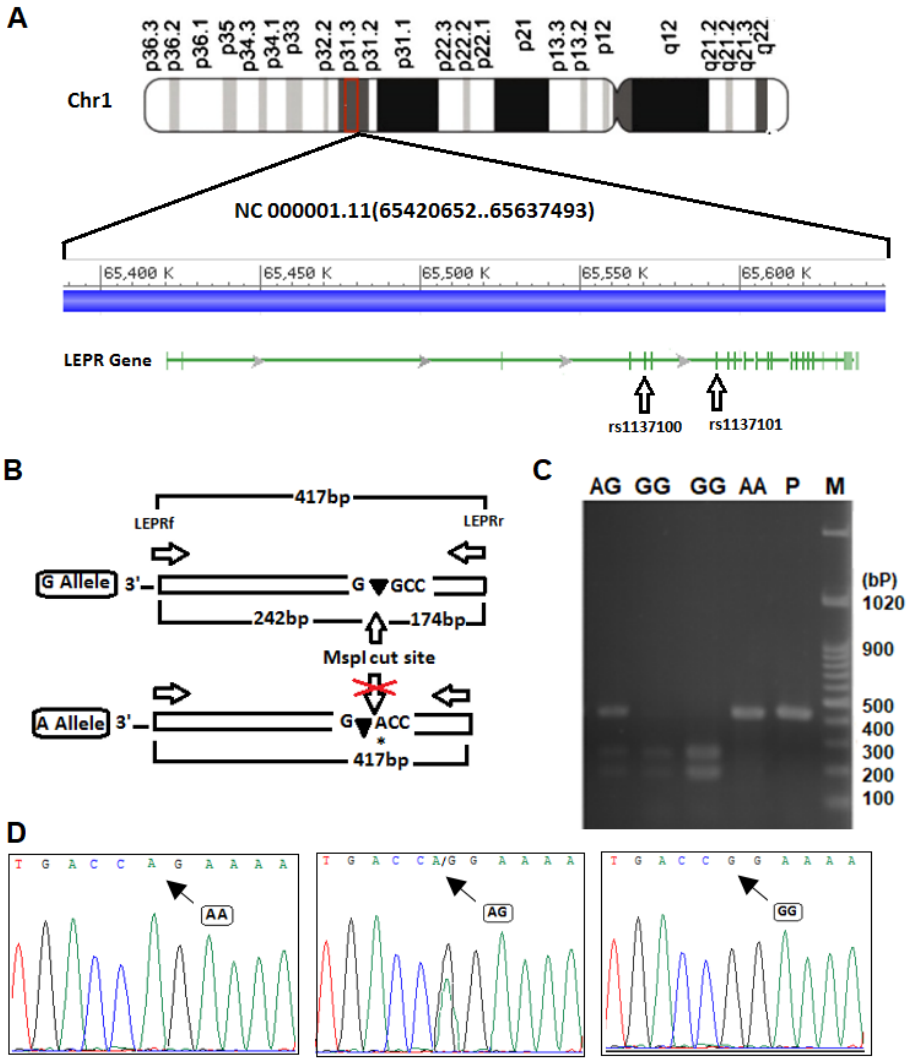

Figure 1. *LEPR* gene map, PCR-RFLP, and DNA sequencing results: (A) Human *LEPR* gene map, from NCBI database, the SNPs of rs1137101 and rs1137100 located in exon7 (position 177266) and exon5 (position 155194), respectively; (B) *Msp*I restriction diagrammatic map of PCR products; (C) *Msp*I restriction map of PCR products in the 1.5% agarose gel electrophorese, which stained by Ethidium bromide, AA, AG and GG lanes indicate genotypes, P= PCR products without *Msp*I restriction enzyme, M= Marker DNA ladder100bp; (D) Electropherogram results of PCR direct sequence which showed genotypes.

Chi-square test was applied to compare the allele and genotype frequencies in the case and control groups. Moreover, Hardy-Weinberg equilibrium (HWE) in both of the case and control groups was tested. The p-value of less than 0.05 was considered as statistically significant. These statistical calculations were performed by SPSS statistical package version 16.

PAGE conditions

Exon 7 PCR fragments were dissected by 12% polyacrylamide gel electrophoresis (PAGE; containing 40 mL polyacrylamide (30%) (29 g, acrylamide:1 g, bis-acrylamide); 5mL of TBE (10X), 350 mL of ammonium persulfate (APS) (10%) and 10 mL of 10% tetramethyl ethylenediamine (TEMED) madeupto100mLwith double-distilled water in 90V for 4h at 48°C with TBE buffer (0.5X). Then, the polyacrylamide gel (12%) was stained with $AgNO_3$. Gel electrophoresis and gel staining were performed according to the methods of Green and Sambrook (2012).

SSCP conditions

For single-strand conformation polymorphism (SSCP) analysis of the 511A>G, PCR products were loaded on 10% polyacrylamide gel and after electrophoresis at 120V for 6 h at 4°C in 1X TBE buffer, visualized by silver nitrate staining based on Green and Sambrook (2012) manual. Preparation of samples for SSCP was performed by 2.5 µl of PCR product which mixed with 7 µl SSCP dye (containing: 9.5 mL Formamide; 400 mL of 20 mM EDTANa2 (pH 8.0) and 100 ml of bromophenol blue

(1%) dissolved in absolute ethanol). This mixture was incubated in the Mastercycler EP for 10 min at 94°C. The samples were then located on a freezer -21°C for 20 min before being loaded in 10% polyacrylamide gel. At least three PCR direct-sequences products were evaluated (Takapouzist Co., Iran) for verification of SSCP results.

In silico analysis

The *in silico* servers were used to describe the possible effects of LEPR (853A>G and LEPR 511A>G) polymorphisms, including the following items: Polyphen2 (http://genetics.bwh.harvard.edu/pph2/): which predicts the probable effects of nsSNPs amino acid on the stability and function of human proteins. HumDiv (human mutation/divergency) and HumVar (human polymorphic variants) are two models on this server (Aftabi et al., 2016); PROVEAN (http://provean.jcvi.org/seq_submit.php): which predicts the effect of replacing the desired amino acid on the biological function of a protein; SNAP (https://www.rostlab.org/services/SNAP/): which is useable for screening of non-acceptable polymorphisms, and predicting the function of mutated protein (Bromberg and Rost, 2007); RNAsnp (http://rth.dk/resources/rnasnp/): which predicts the effect of SNPs on the local RNA secondary structure; dpPTM (http://dbptm.mbc.nctu.edu.tw/index.php): to reports the solvent availability of substrate, protein secondary and tertiary structures, domains and variations (Minguez et al., 2012); Cfssp (http://www.biogem.org/tool/chou-fasman/): for determination of protein secondary structures according to Chou and Fasman algorithm (Chou and Fasman, 1974); ProtParam (https://web.expasy.org/protparam/): to predict the effect of the changes of polymorphism on the primary physicochemical property and the local secondary structure of the protein (Khosronezhad et al., 2015; Aftabi et al., 2016); MUpro (https://www.ics.uci.edu/~baldig/mutation.html): that predicts value and energy change using SVM and sequence information (Cheng et al., 2006); SNPeffect 4.0 (www.snpeffect.switchlab.org): which usually focuses on the molecular specifications and polymorphism types in human proteins (Aftabi et al., 2016); BioGRID (http://thebiogrid.org/): that is a public database which archives and disseminates genetic and protein interplay data from model organisms and human (Chatr-Aryamontri et al., 2014); UbPred (http://www.ubpred.org/help.html): which predicts ubiquitination sites of protein (Radivojac et al., 2010); SUMOplot™ (http://www.abgent.com/sumoplot): that predicts the possibility of the sumo consensus sequence and its score system is according to two standard of the direct amino acid, in compliance with sumo consensus sequence, and substitution of the consensus residues with amino acids exhibiting similar hydrophobicity (Aftabi et al., 2016).

Results

Genotyping of LEPR-853A>G

The *LEPR*-853A>G flanking fragments of samples were amplified by PCR. These 417 base pairs (bp) fragments were run in 1.5% agarose gel. The *Msp*I restriction pattern of PCR products showed three fragments: 417, 243 and 174bp were AG; without cut fragment was AA, and two fragments (243 and 174 bp) were GG genotypes (Figure 1B & 1C). The PCR-RFLP was verified by PCR direct sequencing of DNA sequences (Figure 1D).

Statistical analysis for 853A>G showed that the frequencies of homozygous (GG) and heterozygous (AG) genotypes in the case group were 51.4% and 17.1%, respectively. These frequencies in the control group were 32.8% and 4.28%, respectively. Therefore, there was a statistically significant difference between the control and case groups. The frequencies of genotypes and alleles of the 853A>G polymorphism in the case and control groups are shown in Table 2.

Genotyping of LEPR- 511A>G

For genotyping of *LEPR*- 511A>G transition, at first all samples screened and analyzed by SSCP on the PAGE (Figure 2A). Our results showed that 63 samples were hybrid, which were probably AG carriers. Then PCR products with polymorphic phenotypes were sent for DNA sequencing, which known as PCR directed sequencing and were sequenced by Tcaposis Co., Iran (Figure 2C).

Statistical analysis for 511A>G showed that the frequencies of homozygous (GG) and heterozygous (AG) genotypes in the case group were 70% and 28.57%, respectively. These frequencies in the control group were 30% and 24.28%, respectively. Therefore, there was a statistically significant difference between the control and case groups. The frequencies of genotypes and alleles of the 511A>G polymorphism in the case and control groups are shown in table 2.

Table 2. Genotype and allele frequencies of LEPR 853A>G and 511 A>G in case and control samples

Genotype	No. and percentage		*p-value* [OR (95% CI)]
	Case (n = 70)	Control (n = 70)	
A: *LEPR* 853A>G			
AA	22 (30)	44 (62.8)	-
AG	36(51.4)	23 (32.8)	0.002 [0.319 (0.154–0.664)]
GG	12 (17.1)	3 (4.28)	0.003 [0.125 (0.032–0.489)]
AG+GG	64 (91.42)	183 (261.42)	0.003 [0.391 (0.209–0.732)]
A	84 (60)	40 (57.14)	0.000 [.0338 (0.197–0.578)]
G	54 (38.57)	38 (27.14)	-
B: *LEPR* 511A>G			
AA	8(11.4)	32(45.71)	-
AG	42(70)	21(30)	0.001 [0.57(0.22-0.147)]
GG	20(28.57)	17(24.28)	0.006 [0.34(0.008-0.149)]
AG+GG	60(85.71)	68(61.81)	0.001 [0.32(0.012-0.019)]
A	72(79.28)	81(88.57)	0.009 [0.44(0.054-0.079)]
G	52(37.14)	29(20.71)	

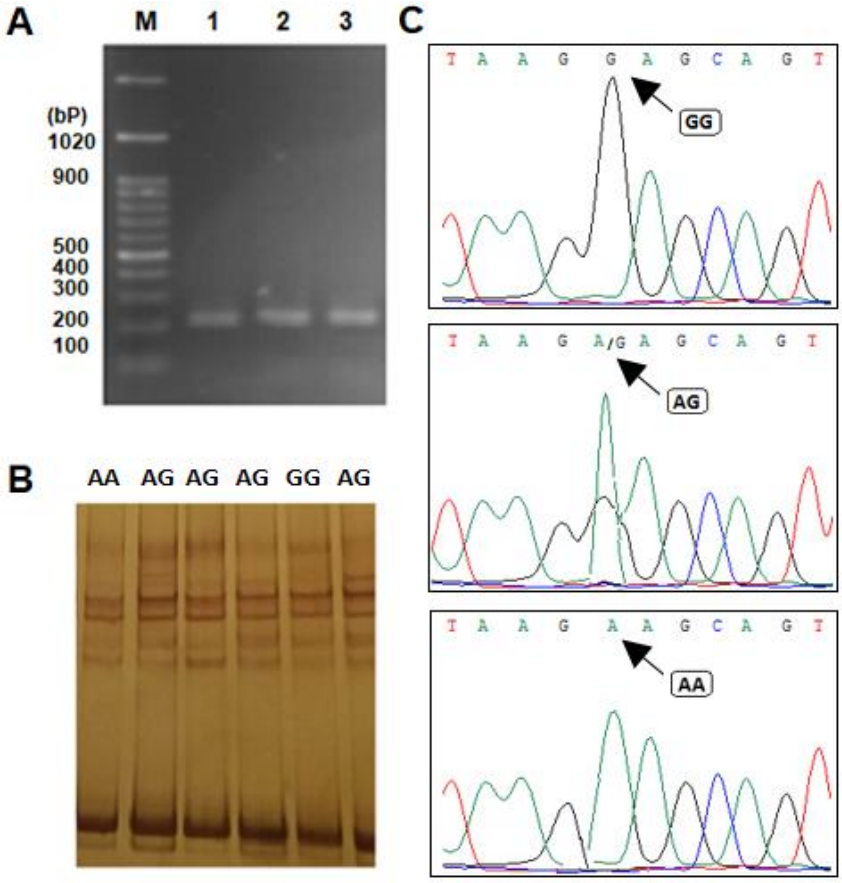

Figure 2. PCR, SSCP, and DNA sequencing results: (A) 217 bp PCR product is shown in 1% agarose gel, M= 100 bp DNA marker; (B) SSCP result shows polymorphic form in polyacrylamide gel; (D) Electropherogram results of PCR direct sequence.

In silico analysis

Polyphen-2 predicted two SNPs, LEPR 853A>G and LEPR 511A>G transition to be benign in both HumDiv and HumVar models analyzing (Figure 3) HumDiv and HumVar scores for 853A>G which are respectively 0.404 and 0.109, and for the 511A>G are 0.077 and 0.021 (Table 3).

The PROVEAN indicated two SNPs, 853A>G and 511A>G substitution as neutral. Variants with a score below -2.5 are considered deleterious and above -2.5 are considered neutral (Choi and Chan et al., 2015). The SNAP server predicted 853A>G and 511A>G mutations are effects (Table 3). The summary of RNAsnp results for LEPR 853A>G and LEPR 511A>G are presented in Table 3. In addition, base pair possibilities of the local region were

Table 3. The result of *in silico* analysis for 853A>G and 511A>G SNPs

Server	Scores			Prediction
[a.] Polyphen-2:				
853A>G	HumVar model: 0.001 (sensitivity: 0.89; specificity: 0.90)			Prediction: Benign
	HumDiv model: 0.000 (sensitivity: 0.91, specificity: 0.69)			Prediction: Benign
511A>G	HumVar model: 0.001 (sensitivity: 0.93; specificity: 0.85)			Prediction: Benign
	HumDiv model: 0.000 (sensitivity: 0.95, specificity: 0.56)			Prediction: Benign
[b.] PROVEAN				
853A>G	Score: -1.404, Prediction Cutoff: 2.5			Neutral
511A>G	Score: -0.478, Prediction Cutoff: 2.5			Neutral
[c.] SNAP				
853A>G	Score: 65, Expected Accuracy:80%			Prediction: effect
511A>G	Score: 38, Expected Accuracy:66%			Prediction: effect
[d.] RNAsnp	Folding Window	Local region	Distance	*p*-value
853A>G	653-1053	806-855	0.0093	0.8132
511A>G	311-711	492-709	0.1532	0.1174

[a]Polyphen-2: predicts the possible impact of nsSNPs derived amino acid substitutions on the stability and function of human proteins employing machine learning classification; [b]PROVEAN: predicts whether an amino acid substitution or indel has an impact on the biological function of a protein; [c]SNAP: is a neural-network based method that uses *in silico* derived protein information in order to make predictions regarding the functionality of mutated proteins; [d]RNAsnp: is a server to predict the effect of SNPs on local RNA secondary structure based on the RNA folding algorithms.

determined with extreme differences located between base pairs 1655 and 1705 (Figure 2A). The p-value more than 0.2, represents a black color region that does not show significant structural changes. Given that amount, the p-value of 0.8132 is for the 853A> G, which does not show a structural change, but p-value equal to 0.1174 for 511A>G, as it is less than 0.2, shows a significant structural change (Figure 2B-C), wild sequences and global mutations (Figure 4D-E).

Dbptm for LEPR-k109 variant predicts the secondary structure of the sequence from the amino acid to the position 109 as a coil and the subsequent sequence from residue 111 to position 119 as a helix that is a normal secondary structure with addition SNP carrying sequence in this position. Also, in LEPR-Q223 predicts secondary structure at position 223 as a sheet and positions 224 to 241 like a coil that is normal. Then, to investigate the effects of SNPs on the secondary structure of the protein, Cfssp was used. Cfssp did not show any difference in the secondary structure in the LEPR K109R as well as in the LEPR Q223R.

ProtParam predictions for the physicochemical properties of the 511A>G and 853A>G are summarized in Table 4. The obtained results are similar for LEPR-K109 and LEPR-Q223, but different for LEPR-R109 in the instability index and gravy and LEPR-R223 in Gravy.

MUpro reported that the K109R and Q223R reduced the stability of the LEPR protein structure with a confidence score which is equal to -0.2 and 0.1, respectively. Also, MUpro prediction of the sign (direction) of energy changes using SVM and NN, decreases the stability of the LEPR protein structure with a confidence score which was equal to -0.1 and -0.5. SNPeffect three predict the effects of nsSNPs on a specification that has important roles in protein folding. TANGO algorithm shows the regional protein sequence. The WALTZ is an algorithm that accurately and specifically predicts amyloid-forming regions in protein sequences. LIMBO algorithm shows chaperone binding site for the Hsp70 chaperones, trained from peptide binding data and structural modeling. The results of the SNP effect for the two polymorphisms 853A>G and 511A>G indicated that dTANGO were equal to -4 and 0, respectively, which meant no change, and dWALTZ was equal to -253, which indicated a decrease and 0 which meant no change. dLIMBO was also for both polymorphisms equal to zero. Moreover, the BioGRID was used to check the network of human LEPR interactions, that defined by physical or genetic experiments. The results of BioGRID is shown in figure 5.

Ubpred predicted the probability of generating proper sumoylation sites after the presentation of K at position 511 and 410. UbPred predicted 10 low configurations, 5 medium confidence and 2 high confidence ubiquitination sites for two SNPs LEPR-K109 and LEPR-Q223. Also, for LEPR-R109 and LEPR-R223, UbPred showed new patterns of ubiquitination, 10 low confidence, 4 medium confidences, and 2 high confidence sites. The SUMOplot ™ analysis predicted 7 low and 7 high probability identical motifs for LEPR-K109 and LEPR-Q223 variants. Furthermore, a different pattern predicted 3 low and 6 highs for LEPR-R109 and LEPR-R223.

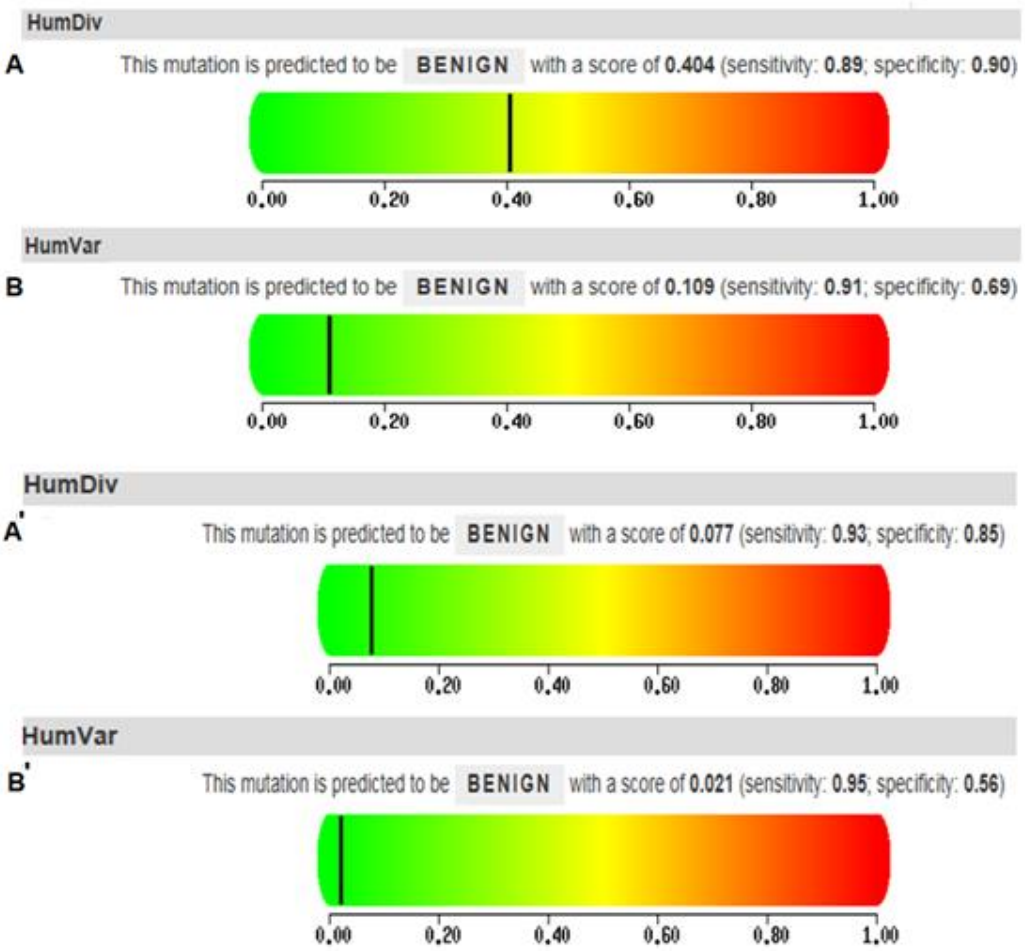

Figure 3. POLYPHEN.2 shows in LEPR-Q223R: HumDiv is sensitivity of 0.89 and in the 0.90 is specificity (A); HumVar is sensitivity of 0.91 and in the 0.69 is specificity and LEPR-K109R (B); HumDiv is sensitivity of 0.93 and in the 0.85 is specificity (A'); HumVar is sensitivity of 0.95 and in the 0.56 is specificity (B').

Discussion

One of the risk factors for pregnancy that causes idiopathic recurrent miscarriage is obesity (Lashen et al., 2004; Jannat Alipoor et al., 2017). Studies by Boots and Stephenson including 24,738 women from four studies, demonstrated that obesity may increase the risk of idiopathic recurrent miscarriage. The percentage of women with one or more miscarriages rose from 10.7% in women with a normal body mass index (BMI) to 11.8% in overweight women and 13.6% in obese women (Bhandari et al., 2016). Leptin is an adipocyte-derived hormone that influences the intake of food and energy consumptions by connecting to specific receptors in the hypothalamus LEPR that is expressed in the brain and hypothalamus, but it is expressed in peripheral tissues such as adipose tissue, liver, kidneys, pancreas, and gonads (Chung et al., 1997; Cohen et al., 2004). LEPR expression in several maternal tissues such as placenta, and fetal tissues indicates the physiologic and pathophysiologic importance of leptin and leptin receptors in normal pregnancy (Sagawa et al., 2002). *LEPR* gene is one of the major genes on the biological pathway of obesity. In 2002, it was shown that expression of LEPR-a and LEPR-b were effective in stimulating LH in rat ovaries (Sagawa et al., 2002). On the other hand, there are some transcription factors that regulate LEPR expression in ovulating granulosa, including nuclear receptor $5a_2$ (Duggavathi et al., 2008), progesterone receptor (Lydon et al., 1995) and CCAAT/enhancer-binding protein (Sterneck et al., 1997). The expression of leptin and leptin receptor in trophoblastic cells indicate that it may increase the activity or synthesis of molecules that regulate trophoblast invasion (Gaus et al., 1997). Placental villi fragments have functional leptin receptors, which stimulate the system A of placental amino acid transport through Janus kinase, signal transporter and activator of transcription proteins signaling pathway.

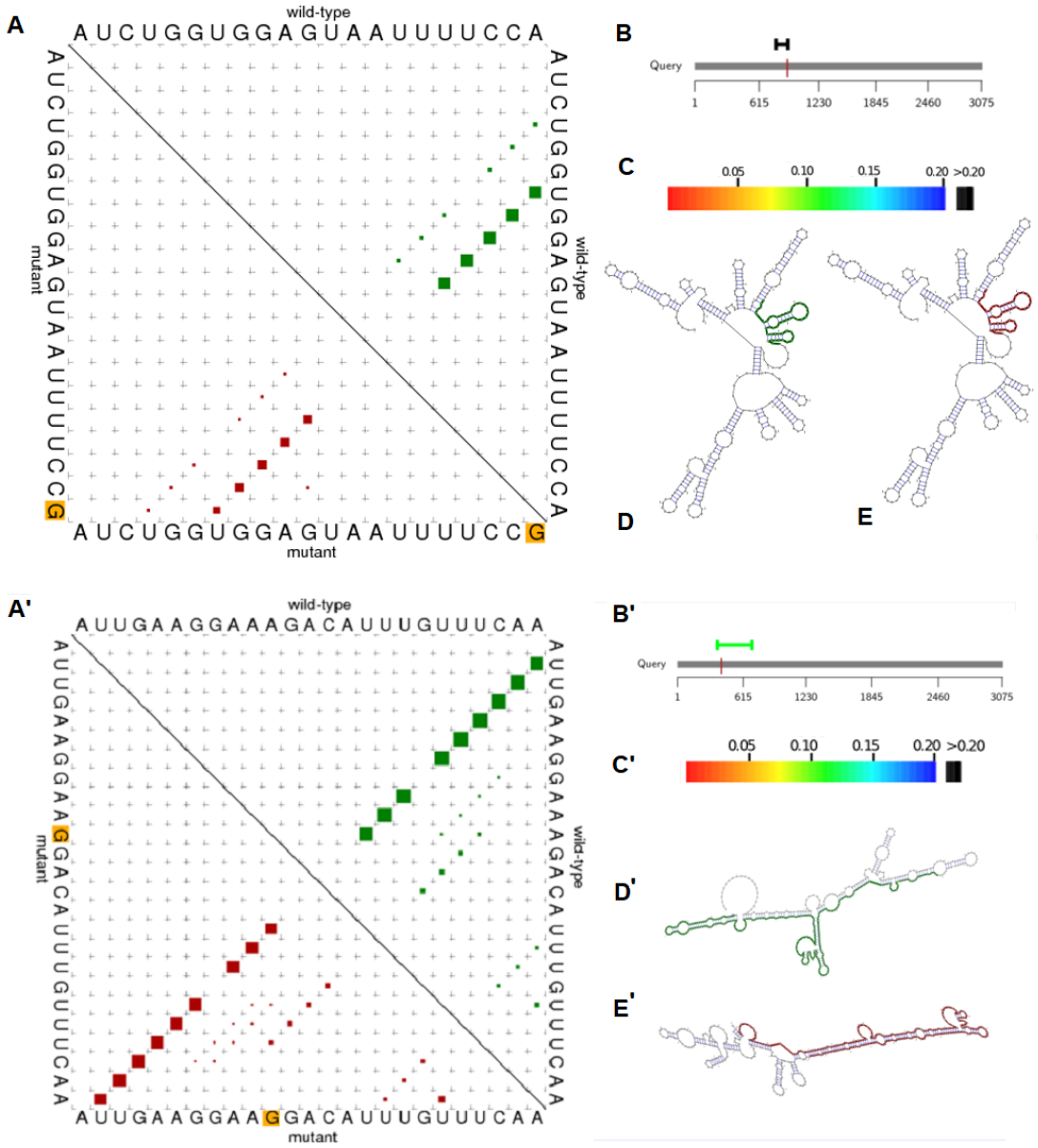

Figure 4. The G1661A and G155194G transitions effects on LEPR-mRNA, analyzed by RNAsnp: RNAsnp analysis of LEPR-853A>G showed from A-D and RNAsnp analysis of *LEPR*- G155194G showed from A'-D', in local region with maximum differences in wild-type and mutant LEPR-mRNA. Base pair probabilities of the local region (653-1053bp for 853A>G, and 492-709 bp for 511A>G) were detected with maximum differences depicted. The upper and lower triangle of the matrix represents the base pair probabilities of wild-type and mutant sequences, respectively. The mutated nucleotide is shown in yellow (A, A'); Graphic summary of the analysis. The SNP-affected region is colored in black since the *p*-value greater than 0.2, which means not very significant change occurred in mRNA structure for 853A>G , and fewer than 0.2, which means very significant change occurred in mRNA structure for 511A>G (B, B'); *p*-value color direction (C, C'); The optimal secondary structure of global wild-type sequence (653-1053) depicted in green with the minimum free energy of -94.40 kcal/mol for 853A>G , and of -76.40 kcal/mol for 511A>G (D, D'); The optimal secondary structure of global mutant sequence, 653-1053, and 492-709, are shown in red with the minimum free energy equals to -93.30 kcal/mol for 853A>G , and -78.50 kcal/mol for 511A>G (E, E').

Placental amino acids transport is decreased in gestation with fetal growth retardation (Jansson et al., 2002). LEPR might have a function in embryo-maternal cross-talk in the implantation window; as in patients with implantation damage role endometrial LEPR expression was lower. Before studies showed, the leptin level in miscarriage women, lower than in those with a successful pregnancy, significantly (Lea et al., 2000; Unkila et al., 2001). Cebpα/β deletions in the granulosa cells restricted human chorionic gonadotropin (hCG), and stimulate to the expression of *LEPR* (Fan et al., 2011). Leptin stimulates the

Table 4. ProtParam-computed physicochemical properties of LEPR-variants.

Variants	Theoretical pI	Extinction coefficients[a]	Instability index[b]	Aliphatic index	Gravy
K109	7.45	[d]198975 Abs 0.1% (=1 g/l) 1.941 and [e]197100 Abs 0.1% (=1 g/l) 1.923	43.53	89.64	-0.107
R109	7.45	[d]198975 Abs 0.1% (=1 g/l) 1.941 and [e]197100 Abs 0.1% (=1 g/l) 1.923	43.62	89.64	-0.108
Q223	7.45	[d]198975 Abs 0.1% (=1 g/l) 1.941 and [e]197100 Abs 0.1% (=1 g/l) 1.923	43.53	89.64	- 0.107
R223	7.45	[d]198975 Abs 0.1% (=1 g/l) 1.941 and [e]197100 Abs 0.1% (=1 g/l) 1.923	43.53	89.64	-0.108

[a] Extinction co-efficients are in units of M-1 cm-1, at 280 nm measured in water; [b]The calculated scores classifies both variants as unstable; [c] Grand average of hydropathicity; [d] Assuming all pairs of Cys residues form cystines; [e] Assuming all Cys residues are reduced.

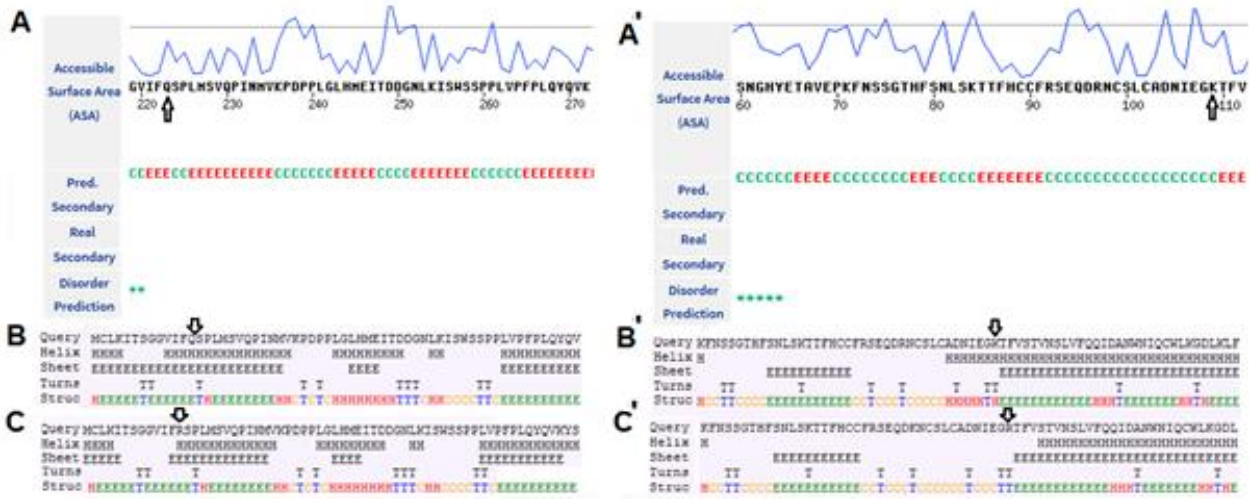

Figure 5. The dbPTM and Cfssp predictions of LEPR-variants structure: The dbPTM prediction of the acidic subdomain structure of LEPR (A, A'); Cfssp predicts a secondary structure for the LEPR-Q223 and LEPR-R109 positions that do not carry the SNP (B, B'); Cfssp predicts a secondary structure for the LEPR-R223 and LEPR-R109 positions that carry the sequence SNP (C, C').

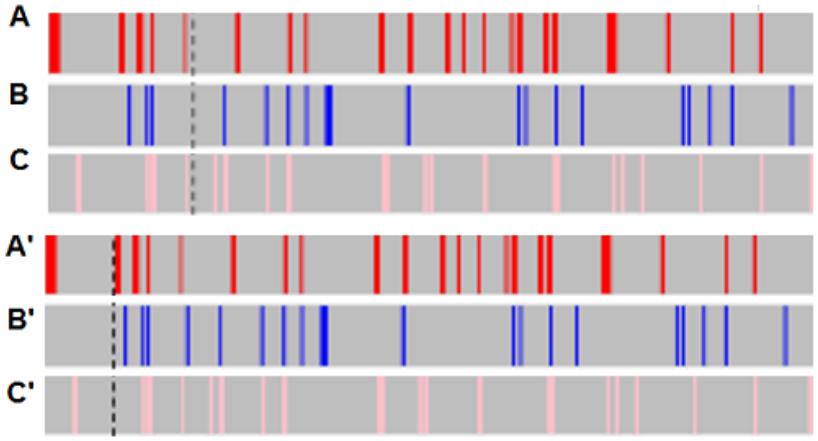

Figure 6. The Q223R and K109R substitutions effects on LEPR-protein folding, analyzed by SNPeffect: In bar representations of the predictions, wild type located on the top and mutant protein in the bottom. The dashed vertical line in the mutant, indicates the positions of the variants residue R223 and R109. The positions of the aggregating stretches visualized in red, blue and pink and it is clear that the variants residue could not disarrange the aggregating stretches; TANGO prediction of aggregation-prone regions (A, A'); WALTZ prediction of amyloid-forming regions (B, B'); LIMBO prediction of chaperone binding sites (C, C').

transport of nutrients to the placenta, which is for fetal growth regulation (Unkila et al., 2001). Some researchers reported that 853A>G *LEPR* gene transition associated with idiopathic recurrent miscarriage (Muller et al., 2016; Riestra et al., 2011), while that this association in Utah (of USA) population not observed (Chin et al., 2013). Since no study on 511A>G *LEPR* gene variants, this SNP as an adjacent SNP with 853A>G *LEPR* gene transition was selected. In this case-control study, we indicated that the AG genotype and G allele were significantly associated with increased risk of idiopathic recurrent miscarriage. We investigated the correlation of 853A>G and 511A>G SNPs in *LEPR* gene with idiopathic recurrent miscarriage in a case-control *in silico* analysis studies to obtain more precise results. Moreover, we performed an *in silico* analysis to demonstrate our findings more accurate. It seems that some single-gene diseases are dependent on missense mutations, especially on non-synonymous single nucleotide polymorphisms (nsSNPs). The effects of nsSNPs on diseases and experimental tests to determine their effects on the structure of related mRNA and protein are usually challenging and difficult. For this purpose, we used *in silico* tools to determine the effects of nsSNPs on protein and mRNA features which may be beneficial in solving these problems (Nouri et al., 2014). To predict the effect of nsSNPs on the protein structure and function, three software (Polyphen-2, PROVEN, SNAP) were used. The results revealed that the 853A>G and 511A>G transitions were benign substitutions without significant effects on the protein structure (Adzhubei et al., 2013). We predicted the secondary structure of mRNA by the RNAsnp server for 853A>G and 511A>G transitions. The data showed that the substitution 511A>G reduced the minimum free energy of the mRNA. Therefore, conferring more stability to LEPR mRNA, may alter the *LEPR* gene expression. However, substitution 853A>G does not reduce the minimum free energy of mRNA (Sabarinathan et al., 2013). Also, the ProtParam server was used to

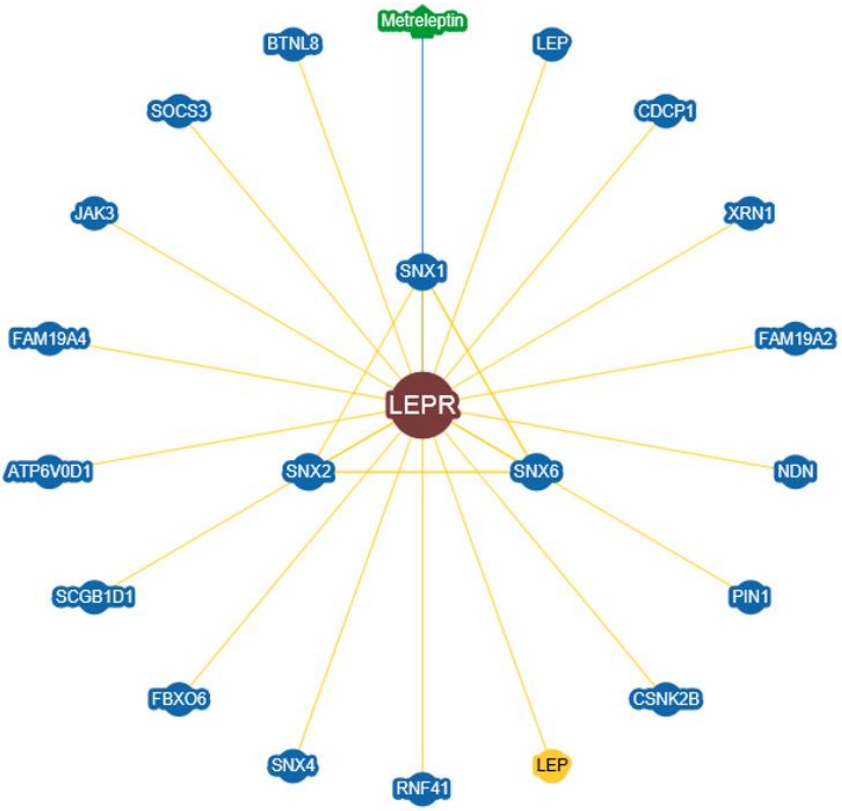

Figure 7. Human LEPR-interactions network obtained from BioGRID: Yellow and purple links demonstrate interactions discovered by physical and genetic experiments respectively; blue links also indicate LEPR-interacted chemicals as well; Proteins: LEP=Leptin; CDCP1= CUB domain-containing protein 1; XRN1= 5'-3' exoribonuclease 1; FAM19A2= Family with sequence similarity 19 member A2; NDN= Named data networking; PIN1= Peptidyl-prolyl cis-trans isomerase NIMA-interacting 1; CSNK2K= Casein kinase; RNF41= E3 ubiquitin-protein ligase NRDP1; SNX4= Sorting nexin-4; FBXO6= F-box only protein 6; SCGB1D1= Segretoglobin family 1D member 1; FAM19A4= Family with sequence similarity 19 Member A4; JAK= Janus kinase 3; SOCS3= Suppressor of cytokine signaling 4; BTNL8= Butyrophilin like8; SNX1= Sorting nexin-1; SNX2= Sorting nexin-2; SNX6= Sorting nexin-6.

determine the physicochemical properties of the LEPR protein. The data indicated that the 853A>G and 511A>G transitions have no effect on the physicochemical features (Gasteiger et al., 2005). We used the dpPTM server to represent the secondary structure of the protein (Lu et al., 2013), and then the CFSSP server to show the effect of SNPs on the secondary structure. The Mupro, reports stability of the LEPR protein, which for both SNPs showed reduced stability (Cheng et al., 2006). Also, BioGRID showed 21 genes involved in LEPR protein (Chatr-Aryamontri et al., 2014). Ubpred predicted changes of ubiquitination sites for two SNPs LEPR-K109 and LEPR-Q223 (Radivojac et al., 2010) and also, for LEPR-R109 and LEPR-R223 as well. The SUMOplot ™ server was used to do sumo sequence analysis for LEPR-K109 and LEPR-Q223.

Conclusions

Based on our findings, LEPR (853A>G and 511A>G) gene transitions may enhance IRM. This notion came about because this loci, as a susceptibility locus, could be used for further case-control studies of IRM. So, these gene transitions might be a useful genetic marker for susceptibility and severity of recurrent miscarriage.

Financial Disclosure

The authors declared no conflicts of interests

Funding/Support

This research is part of the MSc thesis of Masomeh Salehi-Doon, which is supported by a research grant obtained from the University of Mazandaran, Iran.

Acknowledgments

The authors thank all study participants in this case-control study. They are thankful to the clinic staff of "Milad Sari Genetic Detection Center and Razi Hospital (Ghaemshahr, Iran)" for recruiting the case and control volunteers. We are grateful from our colleagues in "Molecular and Cell Biology Research Laboratory of the University of Mazandaran" for critical reviews of the manuscript.

References

Adzhubei I., Jordan D. M. and Sunyaev S. R. (2013) Predicting functional effect of human missense mutations using PolyPhen-2. Current Protocols in Human Genetics 120:301-333.

Aftabi Y., Colagar A. H. and Mehrnejad F. (2016) An in silico approach to investigate the source of the controversial interpretations about the phenotypic results of the human AhR-gene G1661A polymorphism. Journal of Theoretical Biology 393:1-15.

AlShaikh F. S., Finan R. R., Almawi A. W., Mustafa F. E. and Almawi W. Y. (2011) Association of the R67X and W303X non-sense polymorphisms in the protein Z-dependent protease inhibitor gene with idiopathic recurrent miscarriage. Molecular Human Reproduction 18(3):156-160.

Alshaker H., Sacco K., Alfraidi A., Muhammad A., Winkler M. and Pchejetski D. (2015) Leptin signalling, obesity and prostate cancer: molecular and clinical perspective on the old dilemma. Oncotarget 6(34):35556.

Bartha T., Sayed-Ahmed A. and Rudas P. (2005) Expression of leptin and its receptors in various tissues of ruminants. Domestic Animal Endocrinology 29(1):193-202.

Baumann H., Morella K. K., White D. W., Dembski M., Bailon P. S., Kim H. and Tartaglia L. A. (1996) The full-length leptin receptor has signaling capabilities of interleukin 6-type cytokine receptors. Proceedings of the National Academy of Sciences 93(16):8374-8378.

Bhandari S., Ganguly I., Bhandari M., Agarwal P., Singh A., Gupta N. and Mishra A. (2016) Effect of sleeve gastrectomy bariatric surgery-induced weight loss on serum AMH levels in reproductive aged women. Gynecological Endocrinology 32(10):799-802.

Bromberg Y. and Rost B. (2007) SNAP: predict effect of non-synonymous polymorphisms on function. Nucleic Acids Research 35(11):3823-3835.

Chatr-Aryamontri A., Breitkreutz B. J., Oughtred R., Boucher L., Heinicke S., Chen D. and Reguly T. (2014) The BioGRID interaction database: 2015 update. Nucleic Acids Research 43(D1):D470-D478.

Cheng J., Randall A. and Baldi P. (2006) Prediction of protein stability changes for single-site mutations using support vector machines. Proteins Structure Function and Bioinformatics 62(4):1125-1132.

Chin J. R., Heuser C. C., Eller A. G., Branch D. W., Nelson L. T. and Silver R. M. (2013) Leptin and leptin receptor polymorphisms and recurrent pregnancy loss. Journal of the California Perinatal Association 33(8):589.

Chou K. C. (2015) Impacts of bioinformatics to

medicinal chemistry. Journal of Medicinal and Pharmaceutical Chemistry 11(3): 218-234.

Chou P. Y. and Fasman G. D. (1974) Prediction of protein conformation. Journal of Biological Chemistry 13(2):222-245.

Chung W. K., Power-Kehoe L., Chua M., Chu F., Aronne L., Huma Z. and Leibel R. L. (1997) Exonic and intronic sequence variation in the human leptin receptor gene (LEPR). Diabetic Medicine 46(9):1509.

Cleveland R. J., Gammon M. D., Long C. M., Gaudet M. M., Eng S. M., Teitelbaum S. L. and Santella R. M. (2010) Common genetic variations in the LEP and LEPR genes, obesity and breast cancer incidence and survival. Breast Cancer Research and Treatment 120(3):745-752.

Cohen A. W., Hnasko R., Schubert W. and Lisanti M. P. (2004) Role of caveolae and caveolins in health and disease. Physiological Reviews 84(4):1341-1379.

Considine R. V., Sinha M. K., Heiman M. L., Kriauciunas A., Stephens T. W., Nyce M. R., Ohannesian J. P., Marco C. C., McKee L. J. and Bauer T. L. (1996) Serum immunoreactive-leptin concentrations in normal-weight and obese humans. The New England Journal of Medicine 334(5):292-5.

Da Silva Santos T., Ieque A. L., de Carvalho H. C., Sell A. M., Lonardoni M. V. C., Demarchi I. G. and Teixeira J. J. V. (2017) Antiphospholipid syndrome and recurrent miscarriage: a systematic review and meta-analysis. Journal of Reproductive Immunology 85(9):141-179

David A., Razali R., Wass M. N. and Sternberg M. J. (2012) Protein-protein interaction sites are hot spots for disease associated nonsynonymous SNPs. Human Mutation 33(2):359-363.

Dias N. F., Fernandes A. E., Melo M. E. D., Reinhardt H. L., Cercato C., Villares S. M. F. and Mancini M. C. (2012) Lack of mutations in the leptin receptor gene in severely obese children. Arquivos Brasileiros de Endocrinologia & Metabologia 56(3):178-183.

Duggavathi R., Volle D. H., Mataki C., Antal M. C., Messaddeq N., Auwerx J. and Schoonjans K. (2008) Liver receptor homolog 1 is essential for ovulation. Genes & Development 22(14):1871-1876.

Fan H. Y., Liu Z., Johnson P. F. and Richards J. S. (2011) CCAAT/enhancer-binding proteins (C/EBP)-α and-β are essential for ovulation, luteinization, and the expression of key target genes. Molecular Endocrinology 25(2):253-268.

Fraga L. R., Dutra C. G., Boquett J. A., Vianna F. S. L., Gonçalves R. O., Paskulin D. D. and Schuler-Faccini L. (2014) P53 signaling pathway polymorphisms associated to recurrent pregnancy loss. Molecular Biology Reports 41(3):1871-1877.

Gasteiger E., Hoogland C., Gattiker A., Wilkins M. R., Appel R. D. and Bairoch A. (2005) Protein identification and analysis tools on the ExPASy server. In The Proteomics Protocols Handbook (pp. 571-607). Humana press

Gaus G., Funayama H., Huppertz B., Kaufmann P. and Frank H. G. (1997) Parent cells for trophoblast hybridization I: Isolation of extravillous trophoblast cells from human term chorion laeve. Placenta Journal 18:181-190.

Green M. R. and Sambrook J. (2012) Molecular cloning: a laboratory manual. Cold Spring Harbor Laboratory Press, Cold Spring Harbor.

Jannat Alipoor F., Asadi M. H. and Torkzadeh-Mahani M. (2017) Miat LncRNA promotes proliferation of cervical cancer cells and acts as an anti-apoptotic factor. Journal of Genetic Resources 3(2):80-86.

Jansson T., Ekstrand Y., Björn C., Wennergren M. and Powell T. L. (2002) Alterations in the activity of placental amino acid transporters in pregnancies complicated by diabetes. Diabetic Medicine 51(7):2214-2219.

Kar B. and Linda C. B. (2017) Genetic factors associated with recurrent pregnancy loss. American Journal of Obstetrics and Gynecology 7(6):00272.

Khosronezhad N., Hosseinzadeh Colagar A. and Jorsarayi S. G. A. (2015) C26232T mutation in Nsun7 gene and reduce sperm motility in asthenoteratospermic men. Journal of Genetic Resources 1(1):25-30.

Kolte A. M., Bernardi L. A., Christiansen O. B., Quenby S., Farquharson R. G., Goddijn M. and Stephenson M. D. (2015) ESHRE special interest group, Early Pregnancy. Terminology for pregnancy loss prior to viability: a consensus statement from the ESHRE early pregnancy special interest group. Molecular Human Reproduction 30(3):495-498.

Lashen H., Fear K. and Sturdee D. W. (2004) Obesity is associated with increased risk of first trimester and recurrent miscarriage: matched case-control study. Molecular Human Reproduction 19(7):1644-1646.

Lea R. G., Howe D., Hannah L. T., Bonneau O., Hunter L. and Hoggard N. (2000) Placental leptin in normal, diabetic and fetal growth-retarded pregnancies. Molecular Human Reproduction 6(8):763-769.

Lu C. T., Huang K. Y., Su M. G., Lee T. Y., Bretana N. A., Chang W. C. and Huang H. D. (2013) DbPTM 3.0: an informative resource for investigating substrate site specificity and functional association of protein post-translational modifications. Nucleic Acids Research 41(D1): D295-D305.

Lydon J. P., DeMayo F. J., Funk C. R., Mani S. K., Hughes A. R., Montgomery C. A. and O'Malley B. W. (1995) Mice lacking progesterone receptor exhibit pleiotropic reproductive abnormalities. Genes & Development 9(18):2266-2278.

Matthiesen L., Kalkunte S. and Sharma S. (2012) Multiple pregnancy failures: an immunological paradigm. American Journal of Reproductive Immunology 67(4):334-340.

Mehmood M. A., Sehar U. and Ahmad N. (2014) Use of bioinformatics tools in different spheres of life sciences. Journal of Data Mining in Genomics & Proteomics 5(2):1.

Messaoudi S., Hizem S., Al-Sulaiti M. A., Al-Busaidi A. S., Magdoud K., Dendana M. and Mahjoub T. (2013) Contribution of JAK2 and STAT3 variants to the genetic susceptibility of recurrent spontaneous miscarriage in a Tunisian population. Genetic Testing and Molecular Biomarkers 17(1):35-39.

Minguez P., Letunic I., Parca L. and Bork P. (2012) PTMcode: A database of known and predicted functional associations between post-translational modifications in proteins. Nucleic Acids Research 41(D1): D306-D311.

Muhlhauser I., Bender R., Bott U., Jörgens V., Grüsser M., Wagener W. and Berger M. (1996) Cigarette smoking and progression of retinopathy and nephropathy in type 1 diabetes. Diabetic Medicine 13(6):536-543.

Muller A., Wagner J., Hodžić A., Maver A., Škrlec I., Heffer M. and Peterlin B. (2016) Genetic variation in leptin and leptin receptor genes is a risk factor for idiopathic recurrent spontaneous abortion. Croatian Medical Journal 57(6):566-571.

Ng P. C. and Henikoff S. (2006) Predicting the effects of amino acid substitutions on protein function. Annual Review of Genomics and Human Genetics 7:61-80.

Nigro G., Mazzocco M., Mattia E., Di Renzo G. C., Carta G. and Anceschi M. M. (2011) Role of the infections in recurrent spontaneous abortion. The Journal of Maternal-Fetal & Neonatal Medicine 24(8):983-989.

Nouri N., Fazel-Najafabadi E., Behnam M., Nouri N., Aryani O., Ghasemi M. and Sedghi M. (2014) Use of in silico tools for classification of novel missense mutations identified in dystrophin gene in developing countries. Gene 535(2):250-254.

Pang L., Wei Z., Li O., Huang R., Qin J., Chen H. and Chen Z. J. (2013) An increase in vascular endothelial growth factor (VEGF) and VEGF soluble receptor-1 (sFlt-1) are associated with early recurrent spontaneous abortion. PLoS One 8(9): e75759.

Radivojac P., Vacic V., Haynes C., Cocklin R. R., Mohan A., Heyen J. W. and Iakoucheva L. M. (2010) Identification, analysis, and prediction of protein ubiquitination sites. Structure Function and Bioinformatics; 78(2):365-380.

Ramirez M. (2017) Psychology of the Americas: mestizo perspectives on personality and mental health: Volume 126 of Pergamon general psychology series (Goldstein A. P., ed), Elsevier Science.

Riestra P., Garcia-Anguita A., Torres-Cantero A., Bayonas M. J., De Oya M. and Garces C. (2011) Association of the Q223R polymorphism with age at menarche in the leptin receptor gene in humans. Biology of Reproduction 84(4):752-755.

Sabarinathan R., Tafer H., Seemann S. E., Hofacker I. L., Stadler P. F. and Gorodkin J. (2013) The RNAsnp web server: predicting SNP effects on local RNA secondary structure. Nucleic Acids Research 41(W1): W475-W479.

Sagawa N., Yura S., Itoh H., Kakui K., Takemura M., Nuamah M. A. and Fujii S. (2002) Possible role of placental leptin in pregnancy. Endocrine Research Journal 19(1):65-71.

Shahsavari S., Noormohammadi Z. and Karizi S. Z. (2015) Association of kinase insert domain containing receptor (KDR) gene polymorphism/haplotypes with recurrent spontaneous abortion and genetic structure. International Journal of Reproductive Biomedicine 13(12):755.

Shin B., Gunawan O., Zhu Y., Bojarczuk N. A., Chey S. J. and Guha S. (2013) Thin film solar cell with 8.4% power conversion efficiency using an earth-abundant Cu2ZnSnS4 absorber. Progress in

Photovoltaics. European Journal of Obstetrics & Gynecology. Obstetrics & Gynecology and Reproductive Biology 21(1):72-76.

Silver R. M., Branch D. W., Goldenberg R., Iams J. D. and Klebanoff M. A. (2011) Nomenclature for pregnancy outcomes: time for a change. American Journal of Obstetrics and Gynecology 118(6):1402-1408.

Sterneck E., Tessarollo L. and Johnson P. F. (1997) An essential role for C/EBPβ in female reproduction. Genes & Development 11(17): 2153-2162.

Su M. T., Lin S. H. and Chen Y. C. (2011) Association of sex hormone receptor gene polymorphisms with recurrent pregnancy loss: a systematic review and meta-analysis. Fertility and Sterility 96(6):1435-1444.

Unkila-Kallio L., Andersson S., Koistinen H. A., Karonen S. L., Ylikorkala O. and Tiitinen A. (2001) Leptin during assisted reproductive cycles: the effect of ovarian stimulation and of very early pregnancy. Molecular Human Reproduction 16(4):657-662.

Unsal M., Kara N., Karakus N., Tural S. and Elbistan M. (2014) Effects of leptin and leptin receptor gene polymorphisms on lung cancer. Tumor Biology 35(10):10231-10236.

Wang L., Gao P., Zhang M., Huang Z., Zhang D., Deng Q. and Zhou M. (2013) Prevalence and ethnic pattern of diabetes and prediabetes in China in. Journal of the American Medical Association 317(24):2515-2523.

Yan J., Saravelos S. H., Ma N., Ma C., Chen Z. J. and Li T. C. (2012) Consecutive repeat miscarriages are likely to occur in the same gestational period. Reproductive Biomedicine Online 24(6):634-638.

Yang J., Wang Y., Wang X. Y., Zhao Y. Y., Wang J. and Zhao Y. Y. (2017) Adverse pregnancy outcomes of patients with history of first-trimester recurrent spontaneous abortion. BioMed Research International 2017: 4359424.

Zhou Y. and Rui L. (2015) Leptin signaling and leptin resistance. Frontiers of Medicine 7(2):207-222.

Journal of Cell and Molecular Research (2019) 11 (1),37-41 DOI: 10.22067/jcmr.v11i1.82685

Research Article

EZH2 Gene Silencing Can Affect the Expression of miR-155 and TP53INP1

Madjid Momeni-Moghaddam*

Department of Biology, Faculty of Sciences, Hakim Sabzevari University, Sabzevar, Iran

Received 29 August 2019 Accepted 26 September 2019

Abstract

Many genetic, epigenetic, and cellular studies on cancer are underway today, and the completion of the genetic and epigenetic library of cancer could be the way to treat the disease in the future. In this study, we have investigated the parallel gene expression changes of EZH2 and miR-155. So far no study has examined the role of these two factors simultaneously and the results of this study could be useful for further studies. For this purpose, using specific shRNA, the EZH2 gene of HCT116 cells was downregulated and then the changes in expression of the miR-155 were investigated. For gene expression study, Real-time PCR as a standard quantitative method was used. The findings of this study showed that in HCT116 human colon cancer cells, downregulation of miR-155 using shRNA can reduce EZH2 expression and also can promote a significant increase in the expression of TP53INP1 gene. Based on the results, we can emphasize the interaction between these two genes. Importantly, EZH2 downregulation has been able to decrease the amount of miR-155 that has also increased expression in many types of cancers. It may be of interest in epigenetic treatments of colon cancer, because miR-155 can control a very important tumor suppressor gene, TP53INP1.

***Keywords*:** colorectal cancer, EZH2, miR-155, epigenetic, HCT116 cell line

Introduction

Cancer is the cause of many human deaths in all countries of the world, and most types of cancer have a uniform distribution throughout the world (Farnia Ghafouri Sabzevari, Madjid Momeni-Moghaddam. 2014). In all types of cancer, genetic and epigenetic differences can be detected compared to normal cells of the body. Due to changing dietary habits as well as changes in human lifestyle today, colon cancer is one of the most common cancers worldwide and it kills many people every year (Kuipers et al. 2015). For this reason, it is important undoubtedly to fully identify the molecular and cellular processes of colon cancer, and in fact to identify genetic and epigenetic relationships.

Colorectal cancer (CRC), also known as the large intestine cancer, develops in the colon or the rectum (Ragusa et al. 2015). CRC is the third most commonly diagnosed cancer worldwide and the third leading cause of cancer death in both men and women in the US. Based on reported statistics, colorectal cancer accounts for about 10 percent of all cancer deaths in developed countries (Kuipers et al. 2015).

EZH2 (enhancer of zeste homolog 2) is one of the most important genes in colon cancer and increased expression of this gene in several types of cancer including colon cancer (Z. Chen et al. 2018; Jiang et al. 2019). This gene actually produces a product that is the catalytic subunit of the polycomb repressive complex 2 (J.-F. Chen et al. 2016; Z. Chen et al. 2018). Overexpression of EZH2 has been noticed in many types of cancers, including breast, prostate, colon, gastric, lung, and glioma cancers.

MicroRNA (miRNA) is a type of RNA molecule that does not produce a protein product (non-coding RNA), but by having complementary sequences during a specific process it can inhibit mRNA either through ribosomal inhibition or complete RNA degradation (Teymoori and Momeni-moghaddam 2017). Nowadays, it has been found that any alterations in various types of microRNAs are associated with physiological malfunction or cancers (Shojania et al. 2019; Momeni-Moghaddam, Yossefi, and Oladi 2017). There is some evidence that explain the reduced expression of miR-155 in some types of cancers (Yu et al. 2018; N. Li et al. 2019; Y. Li et al. 2018; Zhang, Zhao, and Deng 2013). Physiological roles of miR-155 are including hematopoiesis by directly targeting SOCS1(Bouamar et al. 2015), a negative regulator for IL-2 signaling (Das et al. 2013), immune system miR-155-5p displays a similar

*Corresponding author's E-mail: *m.momeni@hsu.ac.ir*

responsiveness to pathogen stimuli and triggering immune system responses (Etna et al. 2018), inflammation, and reduction of IgG1(Qiu et al. 2018).

MiR-155 today is known as oncomiR and both overexpression and downregulation are detectable based on cell dynamic, so every change of miR-155 can control the expression of its target tumor protein 53-induced nuclear protein 1 (TP53INP1).

The purpose of this study was to investigate the changes in miR-155 and TP53INP1 expression after the suppression of EZH2 expression in cancer cells.

Materials and Methods

Cell culture

HCT116 cells (Pasteur Institute of Iran) were cultured in Dulbecco's Modified Eagle Medium (DMEM), containing 10% fetal bovine serum (FBS) and 1% penicillin-streptomycin. Cells were incubated in a cell culture incubator (Memmert Incubator Oven INB200) with a humidified atmosphere and 5% CO_2 at 37˚C. Culture medium was changed every other day.

Gene Expression Knockdown

EZH2-specific shRNA was redesigned (origin: pSIREN-retroQ-EZH2, Dr.Yutaka Kondo,AICHI,Japan) by Academic Center for Education, Culture and Research (Mashhad, Iran) and synthesized by Macrogen (South Korea). Co-transfections of shRNA vectors, GP and VSV-G plasmids were performed in HEK293T cell line using calcium phosphate-based protocol, and retroviral particles were enriched using ultracentrifugation (beckman centrifuge) for 120 min at 70,000 g, at 4 °C. The HCT116 cells were plated in six-well plates (Nunc™) at a density of 2 × 105 cells per well and were grown overnight until 50–80% confluency to obtain maximum transfection yield. Then lentivirus was added to the wells. The medium was changed 24h after transfection, and the subsequent experiments were performed 72h after transfection. Puromycin (Invitrogen Corporation, Carlsbad, CA) was applied to select infected cells.

Investigation of gene expression

The specific primers for microRNA used in this study were purchased from Exiqon Company (Exiqon, a leading supplier of flexible solutions for RNA research, is now part of QIAGEN), other primers were designed using provided sequence in NCBI and synthesized by Macrogen Company (South Korea). All primers and sequences are listed in Table 1. RNA extraction (Trizol) as well as cDNA synthesis (Bioneer, south korea) were carried out according to the company's protocols. In this study, Trizol (Thermo Fisher Scientific) reagent used for RNA extraction and Cyber-Green II (Amplicon) was used to perform real-time in a thermal cycler (Corbett Research RG 3000).

Table 1. Primers sequences used for real-time PCR

Primer name	Sequences	NCBI Reference Sequence
TP53INP1F	5’-CCA CGTACAATGACT CTTCT-3’	NM_001135 733.2
TP53INP1R	5’-TTCTTGGTTGGA GGAAGAAC-3’	NM_001135 733.2
EZH2F	5’-TTGTTGGCGGAA GCGTGTAAAAT C-3’	NM_004456. 5
EZH2R	5’-TCCCTAGTCCCG CGCAATGAGC-3’	NM_004456. 5
GAPDHF	5’-GGAAGGTGAAG GTCGGAGTCA-3’	NM_002046. 7
GAPDHR	5’-GTCATTGATGGC AACAATATCCA C-3’T	NM_002046. 7

Results

Downregulation of EZH2 Expression

The expression level of EZH2 gene was examined using real-time PCR method. In Figure 1 it has been shown that the level of EZH2 expression was significantly reduced by shRNA compared to non-treated control group (P<0.05). Moreover, there is a significant difference in gene expression between 24 and 48 hours post transfection.

MTT assay

This colorimetric assay was used to determine the proliferation rate of HCT116 cells after downregulation of EZH2 expression. The results confirmed that the number of viable cells in the

treatment groups were significantly decreased at 24, 48, 72 post transfection ($P < 0.05$, Figure-2). These results suggested that the expression level of EZH2 could regulate the rates of cell proliferation and growth (Figure 2).

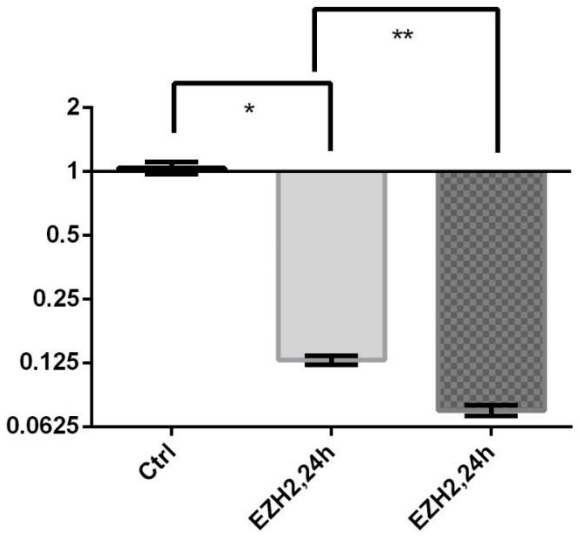

Figure 1. Downregulation of EZH2 expression using its specific shRNA**,** significant decrease of EZH2 expressions have shown after 24 hours and 48 hours compared to control group.

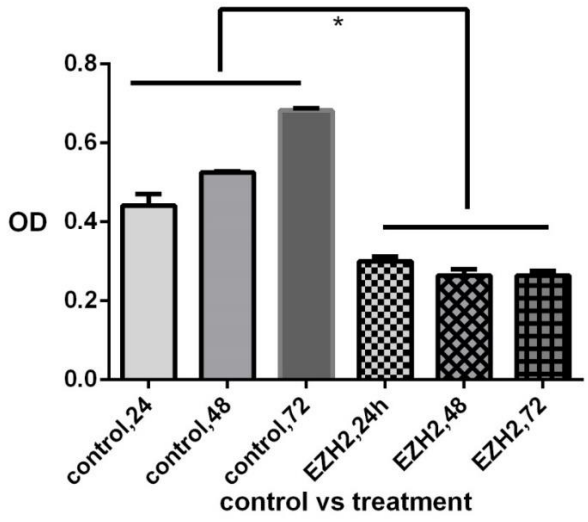

Figure 2. Downregulation of EZH2 expression inhibits the proliferation of HCT116 cells (P <0.05). Curves show the growth of HCT116 cells at 24, 48 and 72 h in control and treatment groups by MTT assay. As shown in the figure, inhibition of EZH2 considerably reduced cell growth.

Molecular findings

RNA extraction was performed for the control and treatment groups and expression of EZH2, miR-155 and TP53INP1 were assessed. As shown in figure-3, a decrease in expression of EZH2 and miR-155 and an increase in expression of TP53INP1 were observed in treatment group (Figure 3).

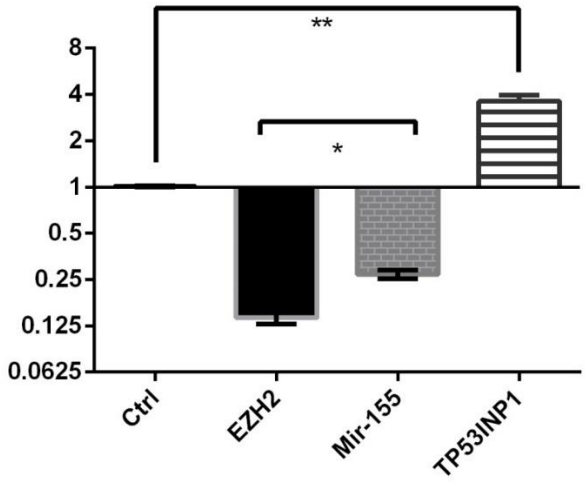

Figure 3. miR-155, EZH2 and TP53INP1 expression in treated and control groups. Level of miR-155 and EZH2 were significantly decreased after 24 h in comparison with control group, but the expression of TP53INP1 compared to control group was significantly increased (P<0.05).

Discussion

In this study, first the EZH2 was downregulated using specific shRNA and then the expression changes of miR-155 and also TP53INP1 were investigated. Although many scientific papers have investigated the role of EZH2 and miR-155 in cancer (Lui et al. 2018; N. Li et al. 2019; Lin et al. 2016; J.-F. Chen et al. 2016), so far, the relationship between these two genes has not been investigated. Hence, finding new information in this area can be important.

The main question was, could we find a synergistic effect between the EZH2 and the miR-155? Did this mean that if we can artificially reduce the EZH2 expression by molecular methods using specific shRNA, will there be a decrease in the second gene?

Given the effect of the EZH2 on the process of cell proliferation, it is clear that any decrease in this gene can lead to a decrease in cell proliferation, which was also tested in this study and confirmed by the MTT assay method. Some articles have clearly mentioned the role of EZH2 on inhibition of apoptosis (Liu et al. 2017).

Researchers have found that any decrease or increase in the expression of miR-155 can have a

completely adverse effect on TP53INP1, indicating that TP53INP1 is regulated by miR-155. In molecular experiments by real-time PCR, these findings were fully confirmed (Seillier et al. 2012; Zhou et al. 2016).

TP53INP1 is a known tumor suppressor, which its expression is downregulated in many types of cancers (Seillier et al. 2012). So, EZH2 not only is a well-known factor in cancer, it can also affect other factors such as TP53INP1 by mediating factors like miR-155.

In conclusion, given that the highly sensitive role of EZH2 and its reduction can lead to decreased gene expression of miR-155 and increased gene expression of tumor suppressor TP53INP1, it could serve as a basis for designing and developing an epigenetic drug to control colon cancer and even other cancers.

Acknowledgements

The authors of this article would like to thank Dr. Moein Farshchian for his efforts in producing the viral particle.

References

Bouamar, Hakim, Daifeng Jiang, Long Wang, An-Ping Lin, Manoela Ortega, and Ricardo C T Aguiar. (2015) MicroRNA 155 Control of P53 Activity Is Context Dependent and Mediated by Aicda and Socs1. Molecular and Cellular Biology 35 (8): 1329–40.

Chen, Jian-Fang, Xi Luo, Li-Sha Xiang, Hong-Tao Li, Lin Zha, Ni Li, Jian-Ming He, Gan-Feng Xie, Xiong Xie, and Hou-Jie Liang. (2016) EZH2 Promotes Colorectal Cancer Stem-like Cell Expansion by ActivatingP21cip1-Wnt/β-Catenin Signaling." Oncotarget 7 (27): 41540–58.

Chen, Zhuanpeng, Ping Yang, Wanglin Li, Feng He, Jianchang Wei, Tong Zhang, Junbin Zhong, Huacui Chen, and Jie Cao. (2018) Expression of EZH2 Is Associated with Poor Outcome in Colorectal Cancer. Oncology Letters 15 (3): 2953–61.

Das, L M, M D L A Torres-Castillo, T Gill, and A D Levine. (2013) TGF-β Conditions Intestinal T Cells to Express Increased Levels of MiR-155, Associated with down-Regulation of IL-2 and Itk MRNA. Mucosal Immunology 6 (1): 167–76.

Etna, Marilena P, Alessandro Sinigaglia, Angela Grassi, Elena Giacomini, Alessandra Romagnoli, Manuela Pardini, Martina Severa, et al. (2018) Mycobacterium Tuberculosis-Induced MiR-155 Subverts Autophagy by Targeting ATG3 in Human Dendritic Cells. PLoS Pathogens 14 (1): e1006790–e1006790.

Farnia Ghafouri Sabzevari, Madjid Momeni-Moghaddam, Faris Farassati and Abolfazl Rad. (2014) Effect of EZH2 Inhibition on Colorectal Cancer Cells: An *In Vitro* Study 6 (8): 289–300.

Jiang, Mingzuo, Bing Xu, Xiaowei Li, Yulong Shang, Yi Chu, Weijie Wang, Di Chen, et al. (2019) O-GlcNAcylation Promotes Colorectal Cancer Metastasis via the MiR-101-O-GlcNAc/EZH2 Regulatory Feedback Circuit. Oncogene 38 (3): 301–16.

Kuipers, Ernst J, William M Grady, David Lieberman, Thomas Seufferlein, Joseph J Sung, Petra G Boelens, Cornelis J H van de Velde, and Toshiaki Watanabe. (2015) Colorectal Cancer. Nature Reviews. Disease Primers 1 (November): 15065.

Li, Ning, Tao Cui, Wenling Guo, Dianwei Wang, and Li Mao. (2019) MiR-155-5p Accelerates the Metastasis of Cervical Cancer Cell via Targeting TP53INP1. OncoTargets and Therapy 12 (April): 3181–96.

Li, Yang, Yanhong Duo, Jiangang Bi, Xiaowei Zeng, Lin Mei, Shiyun Bao, Lisheng He, Aijun Shan, Yue Zhang, and Xiaofang Yu. (2018) Targeted Delivery of Anti-MiR-155 by Functionalized Mesoporous Silica Nanoparticles for Colorectal Cancer Therapy. International Journal of Nanomedicine 13 (March): 1241–56.

Lin, Xiaolin, Yujuan Qin, Junshuang Jia, Taoyan Lin, Xia Lin, Li Chen, Hui Zeng, et al. (2016) MiR-155 Enhances Insulin Sensitivity by Coordinated Regulation of Multiple Genes in Mice. PLoS Genetics 12 (10): e1006308–e1006308.

Liu, Yongfeng, Junjie Peng, Tongyu Sun, Ni Li, Le Zhang, Jiale Ren, Huairui Yuan, et al. (2017) Epithelial EZH2 Serves as an Epigenetic Determinant in Experimental Colitis by Inhibiting TNFα-Mediated Inflammation and Apoptosis. Proceedings of the National Academy of Sciences of the United States of America 114 (19): E3796–3805.

Lui, Julian C, Kevin M Barnes, Lijin Dong, Shanna Yue, Evan Graber, Robert Rapaport, Andrew Dauber, Ola Nilsson, and Jeffrey Baron. (2018) Ezh2 Mutations Found in the Weaver Overgrowth Syndrome Cause a Partial Loss of H3K27 Histone Methyltransferase Activity. The Journal of Clinical Endocrinology and Metabolism 103 (4): 1470–78.

Momeni-Moghaddam, Madjid, Elnaz Yossefi, and Fatemeh Oladi. (2017). MicroRNAs: Small Regulators of Tissue Regeneration. Journal of Genes and Cells 3 (1): 6.

Qiu, Lipeng, Yan Zhang, Danh C Do, Xia Ke, Simin Zhang, Kristin Lambert, Shruthi Kumar, et al. (2018) MiR-155 Modulates Cockroach Allergen- and Oxidative Stress-Induced Cyclooxygenase-2 in Asthma. Journal of Immunology (Baltimore, Md. : 1950) 201 (3): 916–29.

Ragusa, Marco, Cristina Barbagallo, Luisa Statello, Angelo Giuseppe Condorelli, Rosalia Battaglia, Lucia Tamburello, Davide Barbagallo, Cinzia Di Pietro, and Michele Purrello. (2015) Non-Coding Landscapes of Colorectal Cancer." World Journal of Gastroenterology 21 (41): 11709–39.

Seillier, M, S Peuget, O Gayet, C Gauthier, P N'Guessan, M Monte, A Carrier, J L Iovanna, and N J Dusetti. (2012) TP53INP1, a Tumor Suppressor, Interacts with LC3 and ATG8-Family Proteins through the LC3-Interacting Region (LIR) and Promotes Autophagy-Dependent Cell Death. Cell Death and Differentiation 19 (9): 1525–35.

Shojania, Hamid Reza, Madjid Momeni-moghaddam, Seyed-ebrahim Hossini, Mohammad Armin, and Jalal Omrani Bidi. (2019) MicroRNA 155 Downregulation by Vitamin C – Loaded Human Serum Albumin Nanoparticles During Cutaneous Wound Healing in Mice. The International Journal of Lower Extremity Wounds.

Teymoori, Atieh, Mojtaba Teimoori, and Madjid Momeni-moghaddam. (2017) Non-Coding RNAs Could Be New Tools for Cancer Treatment. Journal of Cell and Molecular Research 9: 44–53.

Yu, San-Jian, Liu Yang, Qi Hong, Xia-Ying Kuang, Gen-Hong Di, and Zhi-Ming Shao. (2018) MicroRNA-200a Confers Chemoresistance by Antagonizing TP53INP1 and YAP1 in Human Breast Cancer." BMC Cancer 18 (1): 74.

Zhang, Chun-Mei, Jing Zhao, and Hua-Yu Deng. (2013) MiR-155 Promotes Proliferation of Human Breast Cancer MCF-7 Cells through Targeting Tumor Protein 53-Induced Nuclear Protein 1. Journal of Biomedical Science 20 (1): 79.

Zhou, Xinru, Yong Mao, Jianjie Zhu, Fanyi Meng, Qi Chen, Lihua Tao, Rui Li, et al. (2016) TGF-B1 Promotes Colorectal Cancer Immune Escape by Elevating B7-H3 and B7-H4 via the MiR-155/MiR-143 Axis. Oncotarget 7 (41): 67196–211.

Scientific Reviewers

Maryam Ameri, Ph.D. candidate (Academic Staff in ACECR Khorasan-Razavi Branch, Mashhad, Iran)

Ahmad Reza Bahrami, Ph.D., (Professor of Molecular Biology and Biotechnology), Ferdowsi University of Mashhad, Mashhad, Iran

Hasan Baghshani, Ph.D., (Associate Professor in Faculty of Veterinary Medicine), Ferdowsi University of Mashhad, Mashhad, Iran

Fatemeh Behnam-Rasouli, Ph.D., (Assistant Professor of Cell and Molecular Biology), Ferdowsi University of Mashhad, Mashhad, Iran

Moein Farshchian, Ph.D., (Assistant Professor of Cell and Molecular Biology), ACECR Khorasan-Razavi Branch, Mashhad, Iran

Masoud Fereidoni, Ph.D., (Professor of Physiology), Ferdowsi University of Mashhad, Mashhad, Iran

Farhang Haddad, Ph.D., (Associate Professor of Genetics/Cell Biology), Ferdowsi University of Mashhad, Mashhad, Iran

Aliakbar Haddad-Mashhadrizeh, Ph.D., (Assistant Professor of Cell and Molecular Biology), Ferdowsi University of Mashhad, Mashhad, Iran

Mohammad Reza Housaindokht, Ph.D., (Professor of Biophysical Chemistry), Ferdowsi University of Mashhad, Mashhad, Iran

S. Navid Goftari, Ph.D. candidate of Cell and Molecular Biology, Ferdowsi University of Mashhad, Mashhad, Iran

Zahra Lari, Ph.D., (Plant Physiology), Ferdowsi University of Mashhad, Mashhad, Iran

Saeid Malekzadeh-Shafaroudi, Ph.D., (Associate Professor in Biotechnology and Plant Breeding Department), Ferdowsi University of Mashhad, Mashhad, Iran

Maryam M.Matin, Ph.D., (Professor of Cell and Molecular Biology), Ferdowsi University of Mashhad, Mashhad, Iran

Ali Moghimi, Ph.D., (Professor of Human and Animal Physiology), Ferdowsi University of Mashhad, Mashhad, Iran

Khadijeh Nezhad Shahrokhabadi, Ph.D., (Assistant Professor of Molecular Genetic), Islamic Azad University, Mashhad Branch (IAUM)

MANUSCRIPT PREPARATION

Manuscripts should be prepared in accordance with the uniform requirements for Manuscript's Submission to **"Journal of Cell and Molecular Research".**

Language: Papers should be in English (either British or American spelling). The past tense should be used throughout the results description, and the present tense in referring to previously established and generally accepted results. Authors who are unsure of correct English usage should have their manuscript checked by somebody who is proficient in the language; manuscripts that are deficient in this respect may be returned to the author for revision before scientific review.

Typing: Manuscripts must be typewritten in a font size of at least 12 points, double-spaced (including References, Tables and Figure legends) with wide margins (2.5 cm from all sides) on one side of the paper. The beginning of each new paragraph must be clearly indicated by indentation. All pages should be numbered consecutively at the bottom starting with the title page.

Length: The length of research articles should be restricted to ten printed pages. Short communication should not exceed five pages of manuscript, including references, figures and tables. Letters should be 400-500 words having 7-10 references, one figure or table if necessary. Commentaries and news should also be 800-1000 words having 7-10 references and one figure or table if necessary.

Types of Manuscript: JCMR is accepting original research paper, short communication reports, invited reviews, letters to editor, biographies of scientific reviewers, commentaries and news.

Statement of Human and Animal Rights: Author's should declare regulatory statement regarding the experiments using animals, human cells/tissues that all in vivo experiments have been performed according to the guidelines (explained by WHO, international animal rights federations or your respective institute) to use animals in their research work.

Conflict of Interest Statement: Authors or corresponding author should declare statement of conflict of interest at the last of manuscript.

Manuscript Evaluation Time: All submitted manuscripts will be evaluated and reviewed according to following evaluation schedule.
Pre-Editorial Evaluation: All submitted manuscripts, right after their submission to JCMR will be evaluation by Editors for being according to the journal scope and format. This evaluation can take 2-7 days of submission.
Reviewer's Evaluation: Selected manuscripts after pre-editorial evaluation will be sent to minimum two blind reviewers assigned by Editor-in-Chief. This process may take 21-27 days.
Post Editorial Evaluation: After receiving reviewer's comments, editors evaluate the manuscripts considering the comments and decide their first decision. This process takes 3-5 days and then authors are informed regarding the editorial decision.

GENERAL ARRANGEMENT OF PAPERS

Title: In the first page, papers should be headed by a concise and informative title. The title should be followed by the authors' full first names, middle initials and last names and by names and addresses of laboratories where the work was carried out. Identify the affiliations of all authors and their institutions, departments or organization by use of Arabic numbers (1, 2, 3, etc.).

Footnotes: The name and full postal address, telephone, fax and E-mail number of corresponding author should be provided in a footnote.

Abbreviations: The Journal publishes a standard abbreviation list at the front of every issue. These standard abbreviations do not need to be spelled out within paper. However, non-standard and undefined abbreviations used five or more times should be listed in the footnote. Abbreviations should be defined where first mentioned in the text. Do not use abbreviations in the title or in the Abstract. However, they can be used in Figures and Tables with explanation in the Figure legend or in a footnote to the Table.

Abstract: In second page, abstract should follow the title (no authors' name) in structured format of not more than 250 words and must be able to stand independently and should state the Background, Methods, Results and Conclusion. Write the abstract in third person. References should not be cited and abbreviations should be avoided.

Keywords: A list of three to five keywords for indexing should be included at bottom of the abstract. Introduction should contain a description of the problem under investigation and a brief survey of the existing literature on the subject.

Materials and Methods: Sufficient details must be provided to allow the work to be repeated. Correct chemical names should be given and strains of organisms should be specified. Suppliers of materials need only be mentioned if this may affect the results. Use System International (SI) units and symbols.

Results: This section should describe concisely the rationale of the investigation and its outcomes. Data should not be repeated in both a Table and a Figure. Tables and Figures should be selected to illustrate specific points. Do not tabulate or illustrate points that can be adequately and concisely described in the text.

Discussion: This should not simply recapitulate the Results. It should relate results to previous work and interpret them. Combined Results and Discussion sections are encouraged when appropriate.

Acknowledgments: This optional part should include a statement thanking those who assisted substantially with work relevant to the study. Grant support should be included in this section.

References: References should be numbered and written in alphabetical order. Only published, "in press" papers, and books may be cited in the reference list (see the examples below). References to work "in press" must be accompanied by a copy of acceptance letter from the journal. References should not be given to personal communications, unpublished data, manuscripts in preparation, letters, company publications, patents pending, and URLs for websites. Abstracts of papers presented at meetings are not permissible. These references should appear as parenthetical expressions in the text, e.g. (unpublished data). Few example of referencing patterns are given as follows:

Bongso A., Lee E. H. and Brenner S. (2005) Stem cells from bench to bed side. World Scientific Publishing Co. Singapore, 38-55 pp.

Irfan-Maqsood M. (2013) Stem Cells of Epidermis: A Critical Introduction. Journal of Cell and Molecular Research 5(1): 1-2.

Note: All the reference should be in EndNote format (JCMR EndNote Style is available on JCMR's web site, Author's Guideline)

Tables and Figures: Tables and Figures should be numbered (1, 2, 3, etc.) as they appear in the text. Figures

should preferably be the size intended for publication. Tables and Figures should be carefully marked. Legends should be typed single-spaced separately from the figures. Photographs must be originals of high quality. Photocopies are not acceptable. Those wishing to submit color photographs should contact the Editor regarding charges.

Black Page Charges: There is no black page charges for publication in the Journal of Cell and Molecular Research.

Color Page Charges: All color pages being printed in color will cost 1,000,000 Iranian Rials/page.

JCMR Open Access Policy: Journal of Cell and Molecular Research follows the terms outlined by the Creative Common's Attribution-Only license (CC-BY) to be the standard terms for Open Access. Creative Commons License.

Note: All manuscripts submitted to JCMR are tracked by using "Plagiarism Tracker X" or "small tools" for possible plagiarism before acceptance to JCMR.

Table of Contents

Journal of Cell and Molecular Research

Volume 11, Number 1, Summer 2019